Geoscience Frontiers 10 (2019) 1139–1165

HOSTED BY

Contents lists available at ScienceDirect

China University of Geosciences (Beijing)

Geoscience Frontiers

journal homepage: www.elsevier.com/locate/gsf

Research Paper

Cenozoic basin evolution of the Central Patagonian Andes: Evidence from geochronology, stratigraphy, and geochemistry

A. Encinas [a,*], A. Folguera [b], R. Riffo [a], P. Molina [a], L. Fernández Paz [b,c], V.D. Litvak [b,c], D.A. Colwyn [d], V.A. Valencia [e], M. Carrasco [a]

[a] Departamento de Ciencias de la Tierra, Facultad de Ciencias Químicas, Universidad de Concepción, Víctor Lamas 1290, Concepción, 4030000, Chile
[b] Instituto de Estudios Andinos, Universidad de Buenos Aires, Facultad de Ciencias Exactas y Naturales, Departamento de Ciencias Geológicas, Buenos Aires, Argentina
[c] CONICET-Universidad de Buenos Aires, Instituto de Estudios Andinos Don Pablo Groeber (IDEAN), Buenos Aires, Argentina
[d] Department of Geology & Geophysics, Yale University, 210 Whitney Ave., New Haven, CT, 06511, USA
[e] School of the Environment, Washington State University, Pullman, WA, 99164, USA

ARTICLE INFO

Article history:
Received 26 September 2017
Received in revised form
25 April 2018
Accepted 22 July 2018
Available online 11 August 2018
Handling Editor: R. Damian Nance

Keywords:
Central Patagonian Andes
U-Pb geochronology
Ar-Ar geochronology
Geochemistry
Stratigraphy
Sedimentology

ABSTRACT

The Central Patagonian Andes is a particular segment of the Andean Cordillera that has been subjected to the subduction of two spreading ridges during Eocene and Neogene times. In order to understand the Cenozoic geologic evolution of the Central Patagonian Andes, we carried out geochronologic (U-Pb and $^{40}Ar/^{39}Ar$), provenance, stratigraphic, sedimentologic, and geochemical studies on the sedimentary and volcanic Cenozoic deposits that crop out in the Meseta Guadal and Chile Chico areas (~47°S). Our data indicate the presence of a nearly complete Cenozoic record, which refutes previous interpretations of a hiatus during the middle Eocene–late Oligocene in the Central Patagonian Andes. Our study suggests that the fluvial strata of the Ligorio Márquez Formation and the flood basalts of the Basaltos Inferiores de la Meseta Chile Chico Formation were deposited in an extensional setting related to the subduction of the Aluk-Farallon spreading ridge during the late Paleocene–Eocene. Geochemical data on volcanic rocks interbedded with fluvial strata of the San José Formation suggest that this unit was deposited in an extensional setting during the middle Eocene to late Oligocene. Progressive crustal thinning allowed the transgression of marine waters of Atlantic origin and deposition of the upper Oligocene–lower Miocene Guadal Formation. The fluvial synorogenic strata of the Santa Cruz Formation were deposited as a consequence of an important phase of compressive deformation and Andean uplift during the early–middle Miocene. Finally, alkali flood basalts of the late middle to late Miocene Basaltos Superiores de la Meseta Chile Chico Formation were extruded in the area in response to the suduction of the Chile Ridge under an extensional regime. Our studies indicate that the tectonic evolution of the Central Patagonian Andes is similar to that of the North Patagonian Andes and appears to differ from that of the Southern Patagonian Andes, which is thought to have been the subject of continuous compressive deformation since the late Early Cretaceous.

© 2018, China University of Geosciences (Beijing) and Peking University. Production and hosting by Elsevier B.V. This is an open access article under the CC BY-NC-ND license (http://creativecommons.org/licenses/by-nc-nd/4.0/).

1. Introduction

The Andean Cordillera is the longest and highest subaerial mountain belt formed in a convergent setting. Along the Chilean margin, this range is related to the subduction of the oceanic Nazca and Antarctic plates beneath South America (Mpodozis and Ramos, 1989). Although plate velocities at the trench are rather uniform north of the Nazca-Antarctica-South America triple junction, the Andes show striking latitudinal differences in width, height, and shortening (Mpodozis and Ramos, 1989; Martinod et al., 2010). It appears that the tectonic regimes operating along the Andean range have varied widely along strike and across time. For example, compressional tectonics have dominated the Andes of southern Peru and northern Chile (~15°S–27°S) throughout most of the Cenozoic (Oncken et al., 2006, and references therein), whereas

* Corresponding author.
E-mail address: aencinas@udec.cl (A. Encinas).
Peer-review under responsibility of China University of Geosciences (Beijing).

https://doi.org/10.1016/j.gsf.2018.07.004
1674-9871/© 2018, China University of Geosciences (Beijing) and Peking University. Production and hosting by Elsevier B.V. This is an open access article under the CC BY-NC-ND license (http://creativecommons.org/licenses/by-nc-nd/4.0/).

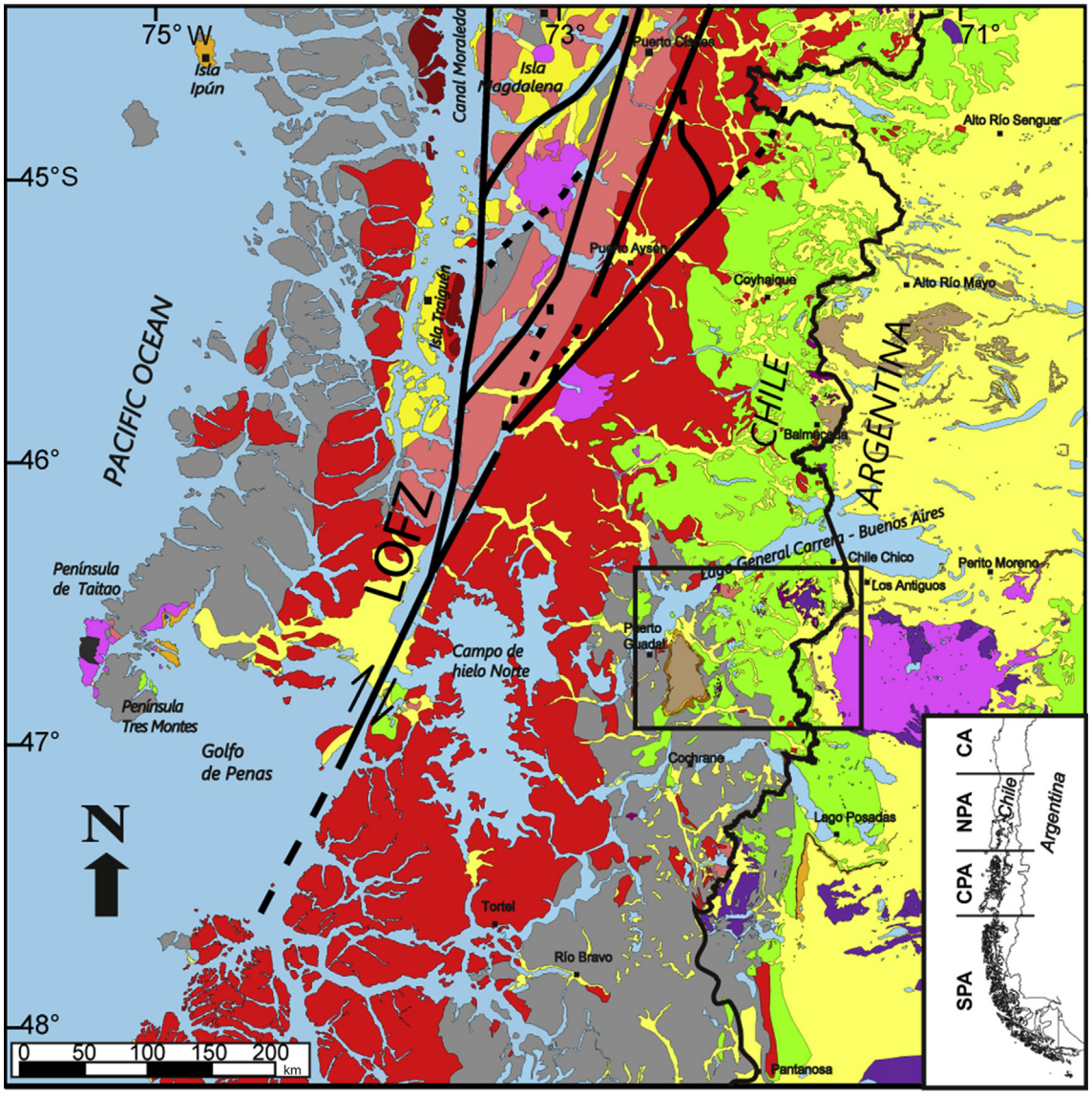

Pleistocene-Holocene volcanic rocks

Pliocene-Holocene glacial, fluvial and marine rocks

Upper Miocene-Pliocene basaltic rocks (BSMCC Formation and equivalent units)

Miocene-Pliocene Taitao Ophiolite.

Lower-Middle Miocene fluvial sedimentary rocks (Santa Cruz Formation and younger units)

Upper Oligocene-Lower Miocene marine volcano-sedimentary rocks (Traiguén Formation)

Upper Oligocene-Lower Miocene marine sedimentary rocks (Guadal Formation, Ipún Formation, Chaicayán group sequence)

Oligocene volcanic, subvolcanic, and plutonic rocks

Eocene basaltic rocks (BIMCC Formation and equivalent units)

Middle Eocene-Upper Oligocene fluvial sedimentary rocks (San José Formation)

Upper Paleocene-Lower Eocene fluvial sedimentary rocks (Ligorio Márquez Formation)

Jurassic-Cretaceous volcanic and sedimentary rocks

Pliocene-Holocene plutonic rocks

Miocene plutonic rocks

Eocene plutonic rocks

Jurassic-Cretaceous plutonic rocks

Paleozoic-Triassic metamorphic rocks

Water bodies ■ Cities and towns Study Area Strike-slip fault

alternating stages of compressional extensional, or neutral tectonics have characterized the Andes of south-central Chile (~33°S–46°S) during the same period (e.g., Mpodozis and Ramos, 1989; Jordan et al., 2001; Charrier et al., 2002; Orts et al., 2012; Encinas et al., 2016a; Horton, 2018b). These temporal and latitudinal changes in the tectonic regime affected not only Andean growth but also other geological characteristics such as the distribution of volcanic centers across the upper plate, the geochemistry of magmatism, the distribution and characteristics of sedimentary basins, and the occurrence of marine transgressions of Pacific and Atlantic origin that have periodically flooded parts of the Chilean margin (e.g., Mpodozis and Ramos, 1989; Jordan et al., 2001).

The causes for these latitudinal and temporal variations in the tectonic regime are debated. The exact mechanism is controversial, as it has been ascribed to different factors such as changes in interplate coupling (Lamb and Davis, 2003; Yanez and Cembrano, 2004), the dip angle of the subducting slab (Martinod et al., 2010), the convergence rate and angle (e.g., Pardo-Casas and Molnar, 1987), or the absolute westward motion of South America (e.g., Silver et al., 1998). Another important process that influences the geologic evolution of convergent margins is the subduction of active oceanic ridges, because they represent first order heterogeneities that affect the tectonic and magmatic development of the upper plate (Scalabrino et al., 2010). Subduction of spreading ridges can cause important effects in crustal deformation and surface morphology (Scalabrino et al., 2010). Their subduction may also lead to the opening of a slab window, which can trigger significant changes in the mantle dynamics beneath the orogenic wedge (Scalabrino et al., 2010, and references therein).

The Central Patagonian Andes at ~47°S (Figs. 1 and 2) is an excellent area to study the geological effects of alternating episodes of compressional and extensional tectonics, as well as the influence of the subduction of spreading ridges on the geological evolution of a convergent margin. This area is of particular interest because it is transitional between a segment of the Andean Cordillera located north of this latitude (~33°S–47°S) that records different periods of extensional and compressional tectonics during the Cenozoic (Muñoz et al., 2000; Charrier et al., 2002; Echaurren et al., 2016) and a segment to the south (47°S–56°S) that is thought to have been subjected to compressive deformation since the Cretaceous (e.g., Biddle et al., 1986). In addition, the triple junction between the Nazca, South American, and Antarctic plates is currently located at this latitude (~47°S), due to northward migration of the subducting Chile spreading ridge during the Neogene. This area previously experienced the subduction of the Aluk-Farallon spreading ridge during the Eocene (Cande and Leslie, 1986). The influence of the subduction of these seismic ridges on the tectonic evolution of the Patagonian Andes during the Cenozoic is debated (Suárez and De La Cruz, 2000; Ramos, 2005). Although there is a general agreement that both episodes of ridge subduction caused the opening of asthenospheric slab windows below the South American plate and the extrusion of extensive flood basalts in Patagonia (Ramos and Kay, 1992; Gorring et al., 1997; Espinoza et al., 2005; Guivel et al., 2006; Breitsprecher and Thorkelson, 2009), there is still no consensus on the deformational influence of these active ridges. Several authors have proposed a relationship between the timing and location of ridge approach and collision and changes in the Patagonian Andes such as rapid mountain uplift and development of a fold and thrust belt (Ramos, 1989; Ramos and Kay, 1992; Flint et al., 1994; Ramos, 2005). However, others have indicated that deformation is not restricted to the time of ridge subduction and expressed doubts about the cause-effect relationship between these two processes (Ray, 1996; Suárez and De La Cruz, 2000). In fact, Suárez et al. (2000), Lagabrielle et al. (2007), and Scalabrino et al. (2010) proposed that the main result of the Chile Ridge subduction has not been compressional deformation, but fast regional uplift related to extensional or transtensional tectonism.

The study of the Cenozoic geological evolution of the Patagonian Andes is hampered by the erosion of most of the Mesozoic–Cenozoic volcano-sedimentary cover, which resulted in extensive exposure of the plutonic and metamorphic basement (Thomson, 2002). However, the hinterland area at ~47°S contains an almost complete Cenozoic record of stratified rocks, which crop out east of the present volcanic arc in the axial part of the Andean Cordillera at Meseta Guadal and in the eastern flank of this chain south of Chile Chico (Niemeyer, 1975; Charrier et al., 1979; Flint et al., 1994; Suárez et al., 2000; De la Cruz et al., 2004; Espinoza et al., 2005; De La Cruz and Suárez, 2006; De la Cruz and Suárez, 2008) (Figs. 1–3). Sedimentary and volcanic rocks in these areas are comprised of upper Paleocene–lower Eocene fluvial strata of the Ligorio Márquez Formation, Eocene flood basalts of the Basaltos Inferiores de la Meseta Chile Chico Formation, middle Eocene–upper Oligocene fluvial strata of the San José Formation, upper Oligocene–lower Miocene marine strata of the Guadal Formation, lower-middle Miocene fluvial strata of the Santa Cruz Formation, and middle-late Miocene flood basalts of the Basaltos Superiores de la Meseta Chile Chico Formation (Fig. 4). The tectonic setting of these strata, which constitute the most complete and well preserved Cenozoic succession of the entire Patagonian Andes, is not well understood, as noted by previous authors (e.g., Suárez and De La Cruz, 2000; De la Cruz et al., 2003). Interestingly, the flood basalts of the Basaltos Inferiores and Superiores de la Meseta Chile Chico formations have been attributed to slab windows opened during the subduction of the Aluk-Farallón and Chile ridges during the Eocene and Miocene respectively (Espinoza et al., 2005). Also relevant is the presence of the marine strata of the Guadal Formation, as they represent the westernmost reach of the late Oligocene–early Miocene Atlantic "Patagonian" transgression that covered most of Patagonia (Niemeyer, 1975; Ramos, 1982; Cuitiño et al., 2015).

In order to understand the geologic evolution of this particular segment of the Andes, we studied the geochronology (U-Pb and $^{40}Ar/^{39}Ar$), provenance, stratigraphy, sedimentology, and geochemistry of the sedimentary and volcanic Cenozoic deposits that crop out in the Meseta Guadal and Chile Chico areas of the Central Patagonian Andes. Using our findings and previous geologic studies in this region, we reconstruct the tectonic setting of this region during the Cenozoic.

2. Geologic setting

There is not a widely accepted latitudinal geological division for the Andean Cordillera of southern Chile and Argentina. Ramos and Ghiglione (2008) proposed a limit between the Central and the Patagonian Andes at 39°S based principally on the presence of a continuous batholith belt that characterizes the southern interval. They farther subdivide the Patagonian Andes in a northern (39°S–43°30′S), central (43°30′S–46°30′S), and southern segments (46°30′S–56°S). Other authors instead define a limit between the Patagonian and the Austral Andes at 47°S (e.g., Melnick et al., 2006). Independently of the classification, there are significant geological differences between the Andean Cordillera north

Figure 1. Regional geologic map. Inset area at Lago General Carrera is shown in Fig. 2. The inset on the right-hand corner shows the divisions of the Andean Cordillera of south-central Chile and Argentina including the southern part of the Central Andes (CA), the Northern Patagonian Andes (NPA), the Central Patagonian Andes (CPA), and the Southern Patagonian Andes (SPA). Figure is after Segemar (1994, 1995), Sernageomín (2003), Ramos and Ghiglione (2008) and Encinas et al. (2016a,b) and references therein. LOFZ–Liquiñe Ofqui Fault Zone.

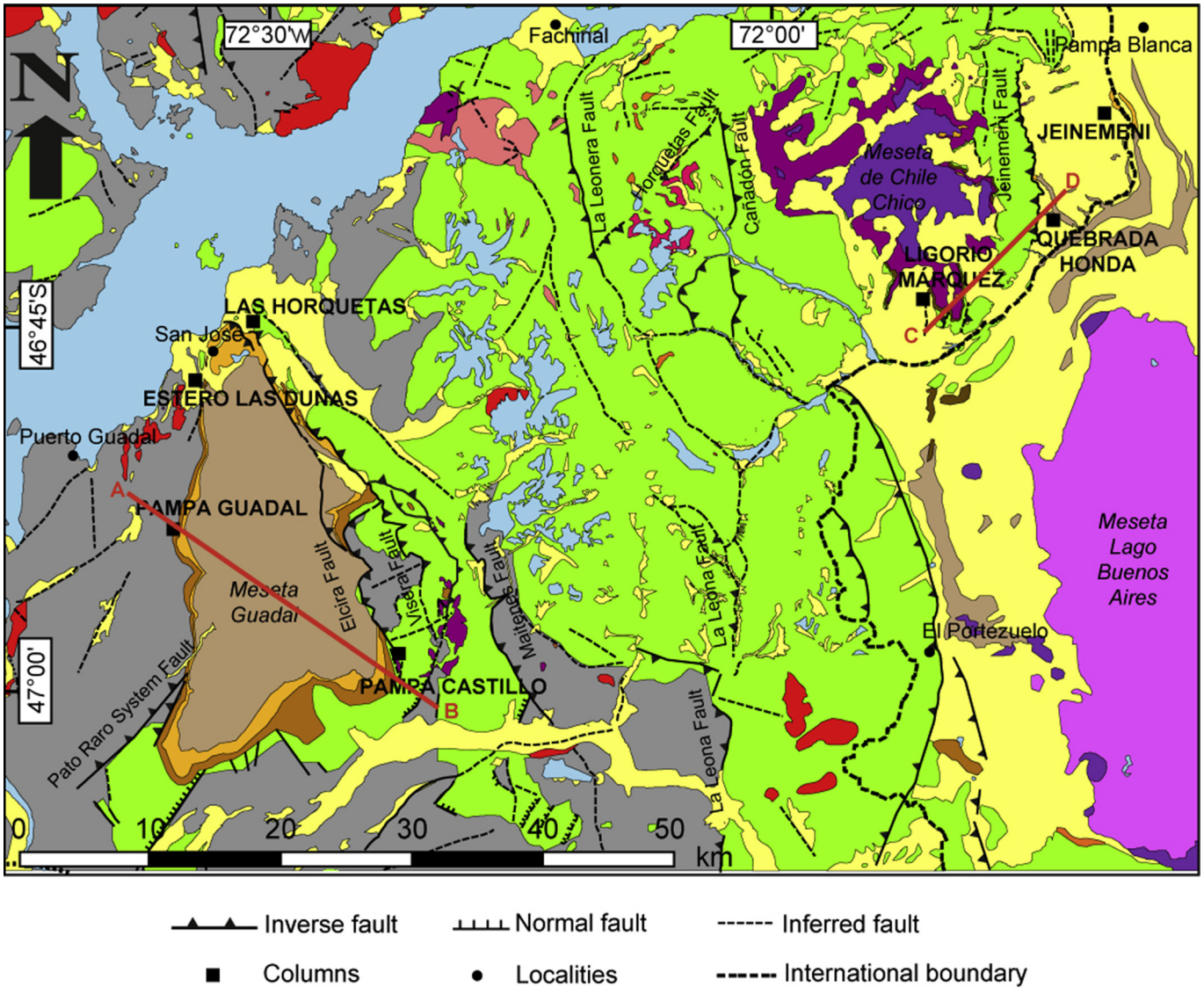

Figure 2. Map of study area showing geologic units and the studied sections (black squares). See Fig. 1 for key to the geologic units.

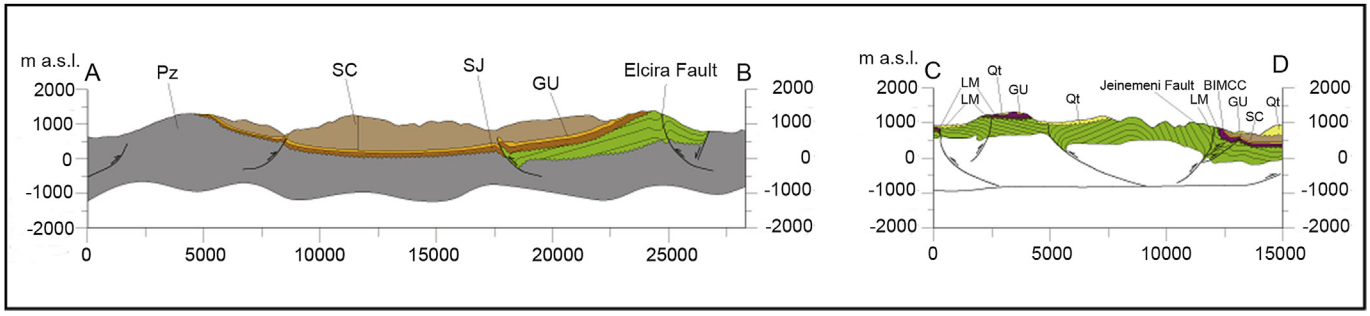

Figure 3. Geological cross section from the Meseta Guadal (A–B) and Meseta Chile Chico (C–D) areas. See location of sections in Fig. 2.

and south of ~47°S. We follow here the division proposed by Ramos and Ghiglione (2008).

Our study area is located in the southern part of the Central Patagonian Andes, in the hinterland area between the present volcanic arc and the eastern limit of this chain (Fig. 1). The most important geologic feature of this segment is the subduction of the Chile Ridge, an active spreading center that forms a triple junction between the Nazca, South American, and Antarctic plates. The Chile Ridge collided with the southern tip of South America (55°S) 14 Ma ago and has since migrated northwards to its present location at the Taitao Peninsula at ~46°S (Cande and Leslie, 1986). The principal geological effects attributed to the subduction of the Chile ridge are

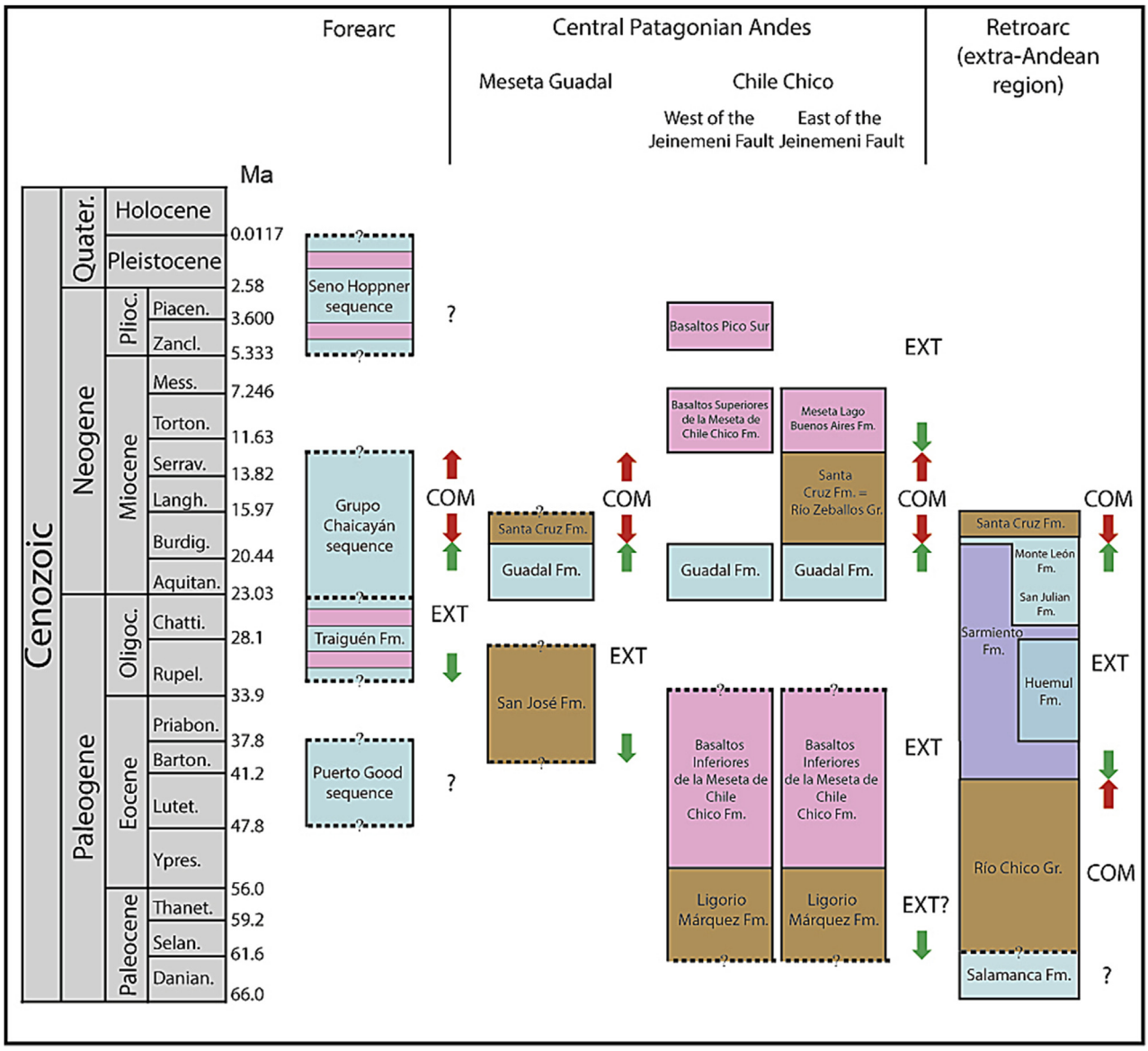

Figure 4. Stratigraphic chart showing the main Cenozoic geological units of the Central Patagonian Andes and those of the forearc and the retroarc at the same latitude. The chart also shows the inferred tectonic contexts for the different areas (see text for further explanation). Colors represent the following kind of sedimentary rocks: marine rocks (blue), fluvial rocks (brown), lava flows (pink), pyroclastic rocks (purple). Red arrows indicate compressional tectonics and green arrows extensional tectonics.

the active opening of an asthenospheric slab window below the South American plate that triggered the extrusion of extensive flood basalts (Ramos and Kay, 1992; Espinoza et al., 2005), subduction erosion of the forearc (Bourgois et al., 1996), emplacement of the Taitao ophiolite (e.g., Mpodozis et al., 1985; Anma et al., 2006), and the occurrence of the highest mountains in the entire Patagonian Andes (Mt. San Valentín, 4058 m a.s.l., and Mt. San Lorenzo, 3706 m a.s.l.) (Lagabrielle et al., 2007). Also attributed to Chile Ridge subduction by most authors is a major N–S-trending, dextral strike-slip fault system referred to as the Liquiñe-Ofqui Fault Zone (LOFZ) (Hervé, 1994). This fault system extends along ~1100 km from 47°S, immediately south of the Chile Triple Junction, to 38°S at the locality of Liquiñe. Its origin is debated, but it has been ascribed to the indenter effect of the Chile Ridge by most authors (Forsythe and Nelson, 1985; Thomson, 2002; Encinas et al., 2013).

The triple junction also marks an important limit in the distribution of geologic units in the Patagonian Andes. North of the triple junction, we can differentiate three distinct belts oriented in an approximately NE–SW direction and characterized by the predominance of different rock units (Fig. 1). From west to east these are: (1) a western belt composed mostly by a Paleozoic–Triassic metamorphic complex (Hervé et al., 2003); (2) a central belt composed, principally, by Jurassic, Cretaceous, Eocene and Miocene plutonic rocks of the Patagonian Batholith (Pankhurst et al., 1999) and less extensively by upper Oligocene–lower Miocene volcano-sedimentary rocks of the Traiguén Formation (Hervé et al., 1995; Encinas et al., 2016a); and (3) an eastern belt, where our study area is located, mostly composed of Mesozoic and Cenozoic sedimentary and volcanic rocks (Suárez and De La Cruz, 2000; Ramos and Ghiglione, 2008). South of the triple junction, the Miocene to Pliocene rocks of the Taitao Ophiolite crop out in the Peninsula Tres Montes (Mpodozis et al., 1985) while a large bay known as the Golfo de Penas extends to the south between 47°S and 48°S. South of the Golfo de Penas, the western belt of Paleozoic–Triassic rocks disappears and the plutonic rocks of the Patagonian Batholith reach the Pacific coast. In addition, south of 47°S the eastern belt is

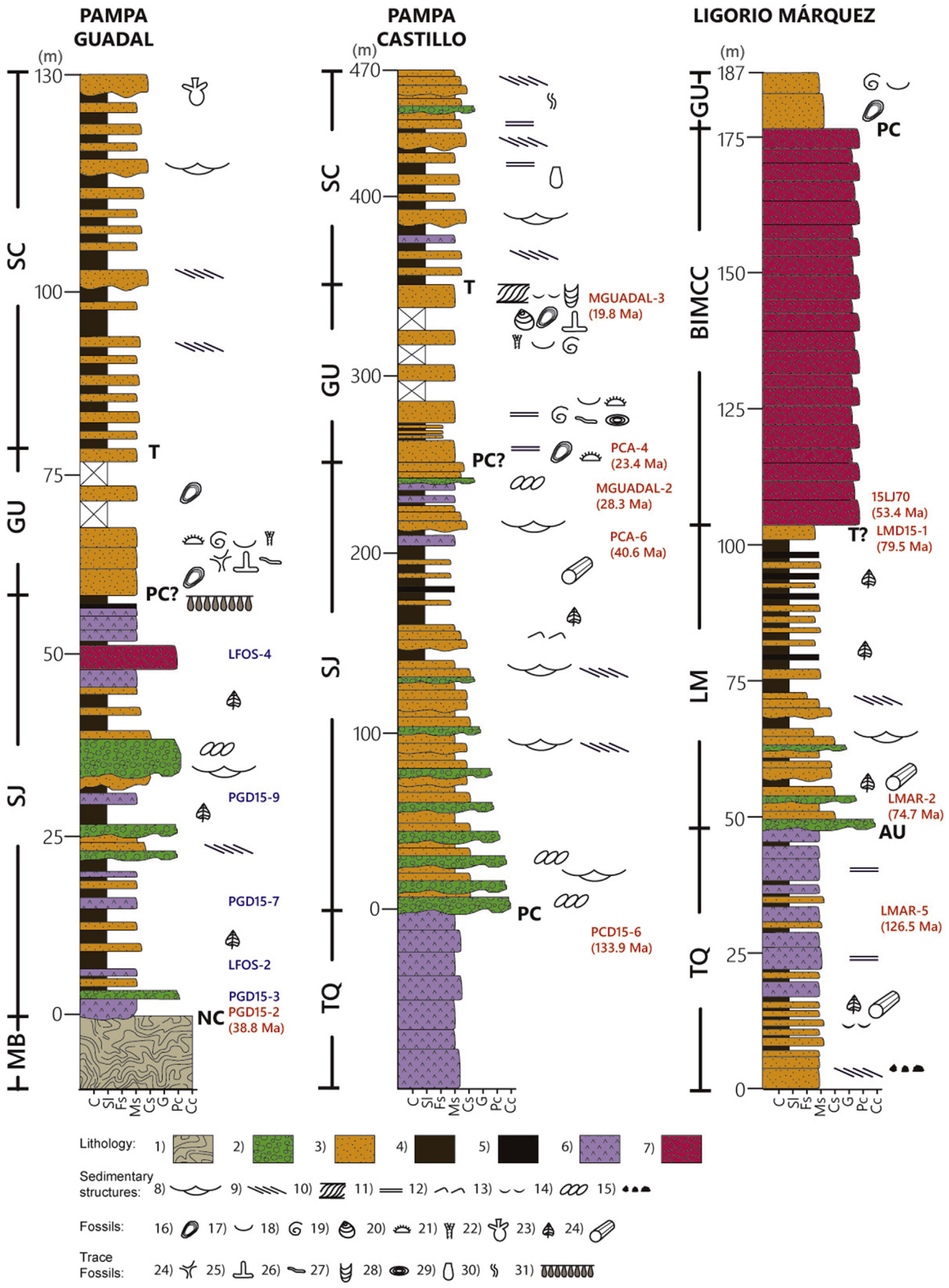
PAMPA GUADAL
(m)
130
100
75
50
25
0
SC
GU
SJ
MB
T
PC?
LFOS-4
PGD15-9
PGD15-7
LFOS-2
PGD15-3
NC
PGD15-2
(38.8 Ma)
C Sl Fs Ms Cs G Pc Cc
PAMPA CASTILLO
(m)
470
400
300
200
100
0
SC
GU
SJ
TQ
T
PC?
PC
MGUADAL-3
(19.8 Ma)
PCA-4
(23.4 Ma)
MGUADAL-2
(28.3 Ma)
PCA-6
(40.6 Ma)
PCD15-6
(133.9 Ma)
C Sl Fs Ms Cs G Pc Cc
LIGORIO MÁRQUEZ
(m)
187
175
150
125
100
75
50
25
0
GUH
BIMCC
LM
TQ
PC
T?
15LJ70
(53.4 Ma)
LMD15-1
(79.5 Ma)
LMAR-2
(74.7 Ma)
AU
LMAR-5
(126.5 Ma)
C Sl Fs Ms Cs G Pc Cc
Lithology: 1) 2) 3) 4) 5) 6) 7)
Sedimentary structures: 8) 9) 10) 11) 12) 13) 14) 15)
Fossils: 16) 17) 18) 19) 20) 21) 22) 23) 24)
Trace Fossils: 24) 25) 26) 27) 28) 29) 30) 31)

dominated by Paleozoic metamorphic rocks (Hervé et al., 2003) and the Meso-Cenozoic cover of sedimentary and volcanic rocks is limited to small outcrops.

In the extra-Andean region, east of the Patagonian Andes, and along the eastern foothills of this chain, early to middle Miocene synorogenic deposits predominate (Lagabrielle et al., 2004; Ramos and Ghiglione, 2008). These rocks are locally overlain by late middle to late Miocene flood basalts (Ecosteguy et al., 2003), and by late Miocene to Quaternary glacial and fluvioglacial deposits (Lagabrielle et al., 2010). In this area, ~200 km east of the Andean Cordillera, a mountain range known as the San Bernardo fold and thrust belt exposes Mesozoic and Cenozoic rocks and constitutes the central part of the 600 km long Patagonian broken foreland (Bilmes et al., 2013; Gianni et al., 2015).

3. Cenozoic stratigraphy

Cenozoic deposits of sedimentary and volcanic origin crop out in the Central Patagonian Andes and the extra-Andean region in eastern Chile and western Argentina. The most complete Cenozoic records occur in the Meseta Guadal and Chile Chico areas (Figs. 1–5). The Meseta Guadal (also known as the Meseta Cosmelli) is an uplifted syncline bounded by reverse faults and located between the Lago General Carrera and the Río Chacabuco (De la Cruz et al., 2004, 2006) (Figs. 1–3). The Meseta Guadal succession constitutes the only record of Cenozoic deposits located near the axial part of the Patagonian Andes. It is comprised of Cenozoic sedimentary and volcanic strata that overlie older Paleozoic and Mesozoic rocks (De la Cruz et al., 2004, 2006). The Cenozoic rocks, from base to top, form a concordant succession including fluvial strata of the San José Formation, marine deposits of the Guadal Formation, and fluvial strata of the Santa Cruz Formation (De La Cruz and Suárez, 2006) (Figs. 2–4). The Chile Chico succession is mostly exposed in a plateau located south of this locality and northeast of Meseta Guadal (Figs. 1–3). The plateau is bounded to the east by a reverse fault referred to as the Jeinemeni Fault and comprises a concordant succession of Cenozoic sedimentary and volcanic strata that overlie Mesozoic rocks (De la Cruz and Suárez, 2008). The Cenozoic record, from base to top, consists of fluvial deposits of the Ligorio Márquez Formation, basaltic rocks of the Basaltos Inferiores de la Meseta Chile Chico (BIMCC) Formation, marine strata of the Guadal Formation, and basaltic rocks of the Basaltos Superiores de la Meseta Chile Chico (BSMCC) Formation (De la Cruz and Suárez, 2008) (Fig. 4). East of the Jeinemeni fault the stratigraphy differs slightly—the Santa Cruz Formation overlies the Guadal Formation and underlies the basalts of the Meseta Lago Buenos Aires Formation, which is correlative with the BSMCC Formation (Ecosteguy et al., 2003; De la Cruz and Suárez, 2008) (Fig. 4). We describe the principal characteristics of the Cenozoic units of the study area in the following section.

3.1. Ligorio Márquez Formation

The Ligorio Márquez Formation is a fluvial succession that crops out at the Chile Chico area (Figs. 2–4). This unit was considered as part of the marine Guadal Formation by Niemeyer (1975). Suárez et al. (2000) separated the fluvial deposits from the marine succession and defined the Ligorio Márquez Formation in the eponymous area southwest of Chile Chico. De la Cruz et al. (2004) correlated the lower part of the fluvial succession at Meseta Guadal with the Ligorio Márquez Formation, but our studies indicate that it corresponds to the younger San José Formation (see section 3.3). The Ligorio Márquez Formation shows an angular unconformity with the underlying Upper Jurassic–Lower Cretaceous strata of the El Toqui Formation (Fig. 6A), a disconformity with Lower Cretaceous strata of the Divisadero Formation and a disconformity with the overlying BIMCC Formation (De la Cruz and Suárez, 2008). The Ligorio Márquez Formation has been classically considered as early Paleocene based on its fossil flora (Troncoso et al., 2002).

The Ligorio Márquez Formation is ~60 m thick and consists of conglomerate, sandstone, mudstone, and coal (Fig. 5). The lower half of the succession is dominated by sandstone and conglomerate with minor intercalations of mudstone and is interpreted as having been deposited in a braided fluvial environment (Fig. 6B). Erosive contacts are common and indicate amalgamation of fluvial channels. Sandstone predominates and shows trough and planar cross-bedding (Fig. 6C). Conglomerates are clast-supported, moderately sorted, and contain cm-scale sub-rounded clasts composed of quartz, tuff, lava, meta-quartzite, and mudstone. Mudstone beds are rarer and typically centimeters to decimeters thick. They contain paleosols, root traces, and fossil leaves and wood. The upper half of the Ligorio Márquez Formation shows facies associations characteristic of a meandering fluvial system. This part of the succession is dominated by floodplain deposits and consists of mudstone, sandstone, and coal (Fig. 6D,E). Fossil leaves and wood are abundant in this interval (Troncoso et al., 2002). Paleocurrent analysis in this unit indicates a SSE direction (De la Cruz and Suárez, 2008).

3.2. Basaltos Inferiores de la Meseta de Chile Chico formation

The BIMCC Formation crops out in the Chile Chico area. This unit was originally defined as the Mantos de Basalto and subsequently correlated with the basalts of the Meseta Lago Buenos Aires Formation that crop out in Argentina (Charrier et al., 1979). Subsequently, it was named as Basaltos Inferiores de la Meseta Chile Chico by Espinoza and Morata (2003) and as Secuencia Basáltica Inferior by Espinoza et al. (2005). Because the first name was used in the geological map of the area (De la Cruz and Suárez, 2008), we follow that designation.

The BIMCC Formation overlies the Ibáñez (Upper Jurassic–Lower Cretaceous), El Toqui (Upper Jurassic–Lower Cretaceous), Divisadero (Lower Cretaceous), and Ligorio Márquez (early Paleocene) formations (Figs. 5 and 6E). The contact with the Mesozoic units has been defined as a disconformity or an angular unconformity by De la Cruz and Suárez (2008). The contact with the Ligorio Márquez Formation is semi-covered but was defined as disconformable by De la Cruz and Suárez (2008). It shows a paraconformity with the overlying Guadal Formation and the BSMCC Formation.

The BIMCC Formation is up to ~350 m thick and consists of basaltic lava flows and minor peridotite xenolith-bearing basanitic necks (Espinoza et al., 2005; De la Cruz and Suárez, 2008). Erupted

Figure 5. Representative sections from the Meseta Guadal (Pampa Guadal and Pampa Castillo sections) and Chile Chico (Ligorio Márquez section) areas (see Fig. 2 for location). Note that vertical scales differ. Acronyms for the different units are: MB: metamorphic basement, TQ: El Toqui Formation, LM: Ligorio Márquez Formation, BIMCC: Basaltos Inferiores de la Meseta Chile Chico Formation, SJ: San José Formation, GU: Guadal Formation, SC: Santa Cruz Formation. Lithology: (1) schist, (2) conglomerate, (3) sandstone, (4) siltstone, (5) coal, (6) tuff, (7) basalt. Sedimentary structures: (8) trough cross-bedding, (9) planar cross-bedding, (10) tidal bundles, (11) parallel lamination, (12) asymmetrical ripples, (13) flaser bedding, (14) imbricated clasts, (15) intraclasts. Fossils: (16) oysters, (17) bivalves, (18) gastropods, (19) brachiopods, (20) echinoderms, (21) bryozoans, (22) vertebrates, (23) leafs (24) wood. Trace Fossils: (24) *Thalassinoides*, (25) *Ophiomorpha*, (26) *Paleophycus*, (27) *Rhizocorallium*, (28) *Asterosoma*, (29) insect traces, (30) undetermined burrows, (31) *Glossifungites* ichnofacies. Grain size: C: clay, Sl: silt, Fs: fine sand, Ms: medium sand, Cs: coarse sand, G: granule gravel, Pc: pebble gravel, Cc: cobble gravel. Contact types: NC: nonconformity, AU: angular unconformity, PC: paraconformity, T: transitional contact.

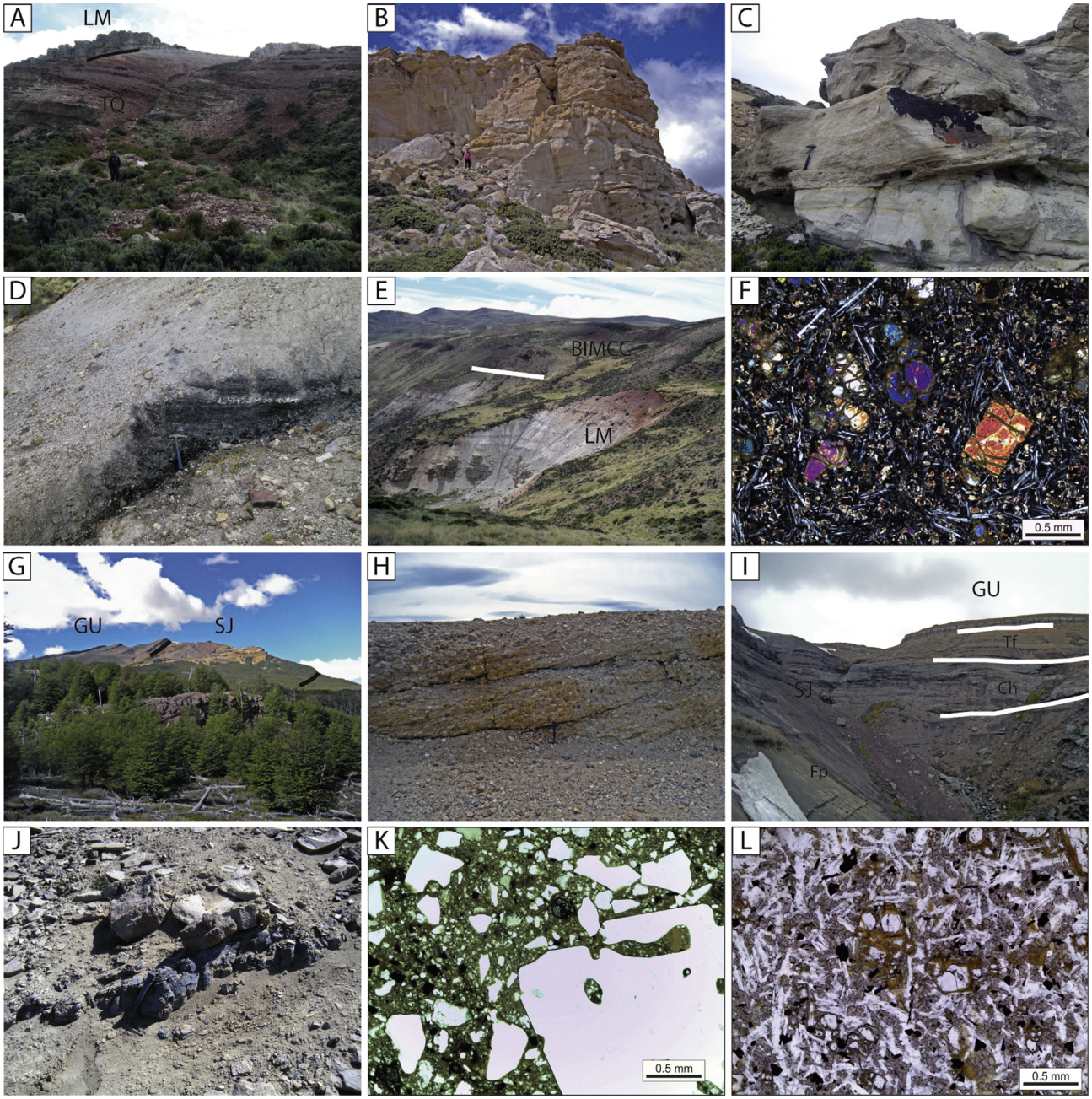

Figure 6. Characteristic features from the Cenozoic deposits of the Meseta Guadal and Chile Chico areas. (A) Angular unconformity between the El Toqui (TQ) and the Ligorio Márquez (LM) formations near Mina Ligorio Márquez, southwest of Chile Chico. Photos B–F are from the same area. (B) Cross-bedded sandstone, minor conglomerate and siltstone from the lower part of the Ligorio Márquez Formation. (C) Detail of cross-bedded sandstones. (D) Detail of coal bed from the floodplain facies of the upper part of the Ligorio Márquez Formation. (E) Concordant contact (covered) between the Ligorio Márquez (LM) and the Basaltos Inferiores de la Meseta Chile Chico (BIMCC) formations. Note predominance of amalgamated channel bodies in the lower part of the Ligorio Márquez Fomation and floodplain facies in the upper part of this unit. (F) Thin section of a basalt from the lower part of the BIMCC Formation showing olivine phenocrysts within a plagioclase, clinopyroxene-rich groundmass. (G) View of the San José (SJ) and Guadal (GU) formations at Pampa Castillo (the Santa Cruz Formation is not visible in this view). (H) Cross-bedded basal conglomerate of the San José Formation at Pampa Castillo. (I) View of the San José (SJ) and basal part of the Guadal (GU) formations at Pampa Guadal. Note floodplain (Fp), channel (Ch) and tuff (Tf) facies associations of the San José Formation, in ascending order. (J) Coal bed from the San José Formation at Pampa Castillo. (K) Crystalline tuff of the San José Formation at Pampa Castillo, showing typical juvenile and embedded quartz fragments in a glassy matrix. This sample (PCA6) was dated at 40.6 Ma. (L) Basalt from the San José Formation at Pampa Guadal (sample LFOS-4) showing olivine phenocrysts within an intergranular groundmass.

rocks consist of nepheline-normative olivine basalts with minor hypersthene-normative tholeiites, trachybasalts and basanites (Espinoza et al., 2005). They have an alkaline and relatively primitive composition and a marked OIB-like signature, reflecting deep mantle origin (Espinoza et al., 2005). Most radiometric ages (K/Ar) for this unit are in the interval 55–40 Ma (see Espinoza et al., 2005 and references therein).

3.3. San José formation

The San José Formation is a fluvial succession that crops out in the Meseta Guadal area (Figs. 2, 3, 5, and 6G) and was considered as part of the marine Guadal Formation by Niemeyer (1975). Flint et al. (1994) defined the San José Formation and separated this unit from the overlying Guadal Formation. Ray (1996) included

the fluvial deposits of the Chile Chico area in the San José Formation. De la Cruz et al. (2004) divided the fluvial succession of Meseta Guadal into a lower Ligorio Marquez Formation and an upper San José Formation based on the presence of more abundant volcanic rocks and clasts in the latter. Our geochronology indicates that the Ligorio Márquez Formation, which was originally defined by Suárez et al. (2000) in the Chile Chico area, is older than the fluvial succession of Meseta Guadal (see sections 4 and 7.1). For this reason, we maintain the name of San José Formation originally proposed by Flint et al. (1994). The San José Formation shows a nonconformity with Paleozoic metamorphic rocks of the Complejo Metamórfico Andino Oriental, an angular unconformity (?) with Upper Jurassic–Lower Cretaceous rocks of the Ibáñez Formation, and a paraconformity with Upper Jurassic–Lower Cretaceous of the El Toqui Formation. It also overlies basaltic volcanic or subvolcanic rocks at the southeastern part of Meseta Guadal that were tentatively assigned to the Eocene by De La Cruz and Suárez (2006). The unit paraconformably or transitionally underlies the Guadal Formation. The San José Formation has been classically considered as lower Eocene based on its fossil flora (De La Cruz and Suárez, 2006).

The San Jose Formation is up to 250 m thick (Fig. 5) and consists of conglomerate (Fig. 6H), sandstone, mudstone, and coal. This unit shows fluvial channel and floodplain facies associations that are typical of meandering fluvial systems (Fig. 6I). Channels are up to 10 m thick, tens of m long, have erosive bases, and consist of fining- and thinning-upward successions of massive and cross-bedded conglomerates and sandstones. Some of these channels show lateral accretion surfaces. Conglomerates are clast-supported, moderately sorted, and contain cm-diameter subrounded clasts composed mostly of quartz, metamorphic rocks, and volcanic rocks. Floodplain facies associations consist of alternating mudstone and sandstone. Beds are typically tabular and decimeters thick. Locally, mudstone strata contain paleosols, root traces, fossil leaves and wood, and coal intercalations (Fig. 6J). In the Pampa Castillo section, the lower part of the San José Formation is dominated by amalgamated channel deposits filled by conglomerate and sandstone, with rare mudstone beds. This part of the succession is interpreted as deposited in a braided fluvial environment. Volcanic tuffs and breccias are sporadically interbedded with sandstones and mudstones in the lower part of the San José Formation. In contrast, volcanic material is dominant in the upper part of this unit where tuff becomes the prevailing lithology (Fig. 6K), with a few intercalations of basaltic rocks (lavas and possible sills) (Fig. 6L), while conglomerates are composed primarily of clasts of andesite, basalt, and pumice. In the uppermost part of the San José Formation at the Pampa Guadal section, we observed a thin coal layer overlain by a siltstone bed below the contact with the overlying Guadal Formation. Paleocurrent analysis in this unit indicates dominantly W and S transport directions (De La Cruz and Suárez, 2006).

3.4. Guadal Formation

The Guadal Formation was originally defined by Heim (1940) as the Mesa Guadal Formation and later renamed by Niemeyer (1975) as the Guadal Formation. This unit crops out at Meseta Guadal and has more limited exposures south of Chile Chico (Niemeyer, 1975; De La Cruz and Suárez, 2006). At Meseta Guadal, the Guadal Formation is paraconformable or transitional with the underlying San José Formation (Figs. 5, 6I and 7A,B) and transitional with the overlying Santa Cruz Formation. In the area south of Chile Chico, the Guadal Formation paraconformably (?) overlies the Paleocene–Eocene BIMCC Formation (Fig. 5), disconformably (?) underlies the BSMCC Formation, and transitionally underlies the Santa Cruz Formation east of the Jeinemeni Fault. Frassinetti and Covacevich (1999) interpreted the fauna of the Guadal Formation as late Oligocene–early Miocene and of Atlantic origin based on its correlation with that of the Monte León Formation of Argentina.

The Guadal Formation is a fossiliferous marine unit up to ~100 m thick that consists of sandstone, siltstone, and minor limestone. This unit contains a rich biota that includes gastropods, bivalves, brachiopods, solitary corals, echinoderms, bryozoans, sharks, whales, and leaves (Frassinetti and Covacevich, 1999; Flynn et al., 2002; De La Cruz and Suárez, 2006) (Fig. 7C–E). The Guadal Formation reflects a transgressive–regressive cycle. The basal contact of this unit shows abundant traces of *Thalassinoides* developed in siltstones from the top of the underlying San José Formation and infilled by sand form the overlying Guadal Formation. This bioturbated horizon is characteristic of the *Glossifungites* ichnofacies (Fig. 7B) and marks the initial stage of the marine transgression. The lower part of the Guadal Formation consists on sandstone and siltstone and shows facies associations indicative of tidal influence and characteristic of estuarine or tidal flat environments. This interpretation (see also Flint et al., 1994; De La Cruz and Suárez, 2006) is based in the presence of tidal bundles, flaser structures, banks of oysters in life position (Fig. 7C), abundant leaves, scarce bioturbation, and a low diversity marine fauna dominated by oysters with minor bivalves and gasteropods. The middle part of the Guadal Formation shows facies associations characteristic of a more open marine environment. They consist of fine-grained sandstones and siltstones that locally show an abundant and diverse biota dominated by bivalves, gastropods, bryozoans, solitary corals, echinoderms, and foraminifera. Sandstones show facies typical of the lower shoreface as they are typically fine-grained, massive, and highly bioturbated showing trace fossils of *Asterosoma* isp., *Rosselia* isp., *Chondrites* isp, *Paleophycus* isp., *Rhizocorallium* isp., and *Planolites* isp. (Fig. 7F). They locally show storm beds composed of disarticulated and broken shells mostly of oysters and secondarily of other species of bivalves and gastropods. Siltstones are massive or laminated and bivalve fossils commonly appear entire and articulated, suggesting preservation in life position or slight transport. These facies are characteristic of shelf deposits dominated by settling processes below storm wave base and represent the maximum depth achieved by the “Patagonian sea” in this region. The upper part of the Guadal Formation is also tidal-dominated, as indicated by the occurrence of mega-ripples, tidal bundles, flaser bedding (Fig. 7G), bimodal paleocurrent directions, scarce bioturbation, oyster banks, and scarce, low-diversity marine fauna.

3.5. Santa Cruz Formation

Early-middle Miocene fluvial synorogenic deposits extend from the Andean front to the Atlantic coast of Patagonia. At the Central Patagonian Andes, these deposits were defined in western Argentina as the Río Zeballos Group by Ugarte (1956) and in Chile as the Río Zeballos Formation by Niemeyer (1975), the Galera Formation by Niemeyer et al. (1984), and the Santa Cruz Formation by De la Cruz et al. (2004) and De la Cruz and Suárez (2008). Although the stratigraphy of these continental deposits needs to be refined, we will use the name Santa Cruz Formation proposed by De la Cruz et al. (2004) and De la Cruz and Suárez (2008). The Santa Cruz Formation transitionally overlies the Guadal Formation at Meseta Guadal (Figs. 5 and 7H) and in the Chile Chico area, east of the Jeinemeni Fault. At this locality, it shows an angular unconformity with the overlying late Miocene–Pliocene basalts of the Meseta Lago Buenos Aires Formation, whereas at Meseta Guadal the top of this formation is not exposed.

The Santa Cruz Formation is up to ~1000 m thick (De la Cruz et al., 2004) and consists of sandstone, mudstone, and minor

Figure 7. Characteristic features from the Cenozoic deposits of the Meseta Guadal and Chile Chico areas (continuation). (A) Concordant contact between the San José (SJ) and Guadal (GU) formations at Estero Las Dunas. (B) Detail of the contact showing *Thalassinoides* ichnospecies (Th) developed in siltstones of the San José Formation and infilled by sand form the overlying Guadal Formation. This bioturbated horizon is characteristic of the *Glossifungites* ichnofacies. (C) Oyster bank at the basal part of the Guadal Formation at Las Horquetas. (D) Bivalves and echinoderm (left of the coin) of the Guadal Formation at Pampa Castillo. (E) Echinoderm of the Guadal Formation at Pampa Castillo. (F) Highly bioturbated sandstone of the Guadal Formation at Pampa Castillo. (As) *Asterosoma* isp. (Ph) *Paleophycus* isp. (G) Flaser bedding in strata of the upper part of the Guadal Formation at Pampa Castillo (H) Transitional contact between the Guadal (GU) and the Santa Cruz (SC) formations at Pampa Castillo. (I) Sandstones and siltstones of the Santa Cruz Formation at Quebrada Honda, Chile Chico area. Note channel sandbodies and a dike crosscutting the sedimentary successions. (J) Detail of channel sandbody (base indicated by arrow) and floodplain facies. Note dark-colored paleosoil below the contact. (K) Detail of root traces from floodplain silty facies. (L) Detail of insect trace, probably *Celliforma* or *Fictovichnus*.

conglomerate and tuff. This unit presents fluvial channel and floodplain facies associations that are typical of meandering fluvial systems. Channel deposits consist of lenticular bodies a few meters thick and 10s of meters long that show erosive bases (Fig. 7I and J). These channel bodies are composed of sandstone and conglomerate with trough and planar cross-bedding, and parallel lamination. Conglomerate is scarcer than sandstone, clast-supported, moderately sorted, and contains sub-rounded clasts centimeters in diameter composed of quartz, volcanic rocks, and minor mudstone intraclasts. Floodplain deposits are predominant in the lower part of the Santa Cruz Formation and consist of interbedded sandstone and mudstone. Beds are typically tabular, laterally continuous, and decimeters thick. Mudstone beds contain paleosols (Fig. 7J), root traces (Fig. 7K), diagenetic concretions, insect traces (Fig. 7L), and locally fresh-water bivalves of the *Diplodon* genus (De La Cruz and Suárez, 2006). Sandstones are typically massive or contain asymmetric ripple marks

and locally present abundant terrestrial vertebrate fossils. Tuff beds are evenly intercalated in floodplain deposits. This unit shows synorogenic growth strata (Lagabrielle et al., 2004; De La Cruz and Suárez, 2006). The Santa Cruz Formation at Meseta Guadal has been assigned to the early Miocene based on the presence of vertebrate fossils characteristic of the Santacrucian SALMA (Flynn et al., 2002). Radiometric dating of the Santa Cruz Formation and younger synorogenic units in the Central and Southern Patagonian Andes indicate an age range between ~19 Ma and 12 Ma (De Iuliis et al., 2008; Rivas et al., 2015; Suárez et al., 2015; Cuitiño et al., 2016; Encinas et al., 2016b). Paleocurrent analysis in this unit indicates an ESE transport direction (De La Cruz and Suárez, 2006).

3.6. Basaltos Superiores de la Meseta Chile Chico Formation

The BSMCC Formation crops out in the Chile Chico area. It was originally correlated with the basalts of the Meseta Lago Buenos Aires Formation (Charrier et al., 1979; Niemeyer et al., 1984) and subsequently named as the Upper Basaltic Sequence (Espinoza et al., 2005). De la Cruz and Suárez (2008) redefined this unit as the Basaltos Superiores de la Meseta Chile Chico Formation. The BSMCC Formation disconformably (?) overlies the late Oligocene–early Miocene Guadal Formation and conformably underlies the Pliocene Basaltos Pico Sur Formation (De la Cruz and Suárez, 2008). The formation is up to ~350 m thick and consists principally on basaltic lava flows and necks (Espinoza et al., 2005; De la Cruz and Suárez, 2008). Erupted rocks are basalts, basanites, trachybasalts, basaltic trachyandesites, and rhyolites, mostly nepheline- and olivine-normative and minor hypersthene-normative (Espinoza et al., 2005). Geochemically, basalts show mostly alkaline and tholeiitic compositions, whereas rhyolites belong to the high-K calc-alkaline series (Espinoza et al., 2005). Mafic lavas of this unit show an OIB-like signature, which reflects a deep mantle origin for these primitive magmas (Espinoza et al., 2005). Most published radiometric ages for the BSMCC range between 12 Ma and 7 Ma (De la Cruz and Suárez, 2008 and references therein), with one single older age of 16.0 ± 0.5 Ma (Charrier et al., 1979).

4. U-Pb geochronology

In order to improve the chronological framework for the deposition and provenance of the Cretaceous and Cenozoic units that crop out at the Meseta Guadal and Chile Chico areas, we carried out U-Pb geochronology on nine samples of sedimentary and volcanic rocks, including sandstones, conglomerates, and tuffs from the El Toqui, Ligorio Márquez, San José, and Guadal formations.

4.1. Analytical method

Zircon crystals from the selected samples were extracted at ZirChron LLC, Tucson AZ, following traditional mineral separation methods. Zircons from the non-magnetic fraction and standards were mounted in a 1-inch diameter epoxy puck and slightly grinded and polished to expose the surface while keeping as much material as possible for laser ablation analyses. After CL imaging, LA-ICP-MS U-Pb analyses were conducted at Washington State University using a New Wave Nd:YAG UV 213-nm laser coupled to a ThermoFinnigan Element 2 single collector, double-focusing, magnetic sector ICP-MS. Operating procedures and parameters were similar to those described in detail in Chang et al. (2006) and Gaschnig et al. (2010). Laser spot size, fluence, and repetition rate were 30 μm, 7 J/cm^2 and 10 Hz, respectively. He and Ar carrier gases delivered the sample aerosol to the plasma. Each analysis consists of a short blank analysis followed by 250 sweeps through masses 202, 204, 206, 207, 208, 232, 235, and 238, taking approximately 30 s. Time-independent fractionation was corrected by normalizing U/Pb and Pb/Pb ratios of the unknowns to the zircon standards (Chang et al., 2006). U and Th concentrations were monitored by comparing to 91500 zircon standard. Two zircon standards were used: Plesovice, with an age of 338 Ma (Sláma et al., 2008) and Fish Canyon Tuff, with an age of 28.4 Ma (Schmitz and Bowring, 2001). Common Pb was corrected using the ^{207}Pb method (Williams, 1998). U-Pb zircon ages were calculated as follows, the youngest age group was recognized (more than three analyses overlapping within the error, Gehrels et al., 2006). Then the ^{206}Pb/^{238}U age was calculated from this group using the TuffZirc algorithm (Isoplot, Ludwig, 2003). Age errors were reported using the propagation of errors of quadratic sum of the analytical error plus the systematic error for that set of analyses (Valencia et al., 2005). Analyses rejected from the TuffZirc algorithm because they are significantly younger or older, were discarded from the age calculation.

4.2. Results

In order to determine the age and zircon provenance of volcanic and sedimentary rocks we analyzed ~50 to 100 zircon crystal per sample respectively. Results from the LA-ICPMS zircon U-Pb isotope analyses are presented in Table DR1. The calculated age of sandstones and conglomerates is considered the maximum depositional age. After a careful petrographic study of the tuffs we interpret them to be primary pyroclastic deposits with no reworking, therefore we consider their calculated age as the age of the magmatic event. Their main petrographic features include angular crystal fragments, juvenile quartz fragments with embayments, corrosion features between the crystals and the matrix, and an exclusively vitreous matrix with no epiclastic components. A summary of the calculated ages determined by ^{206}U/^{238}Pb Tuffzirc ages and other age groups are presented in Table 1. Probability density age distribution and TuffZirc age plots are presented in Figs. 8 and 9. Location of samples within the stratigraphic columns is indicated in Fig. 5.

Zircons from these samples are clear and colorless. They display a variety of morphologies, but are mainly long euhedral crystals dominated by long, prominent bi-pyramidal terminations; minor proportions of subhedral to subrounded zircon crystals are present. Cathodoluminescence images show oscillatory to sector zoning, indicating a simple growth history.

We collected a tuff sample (PCD15-6) from strata of the upper part of the El Toqui Formation at the Pampa Castillo section in Meseta Guadal. The sample yielded age of ~134 ± 2 Ma (n = 22 of 48). Older single ages ranging from 454 Ma to 1199 Ma probably correspond to recycled zircons derived from the metamorphic basement.

Sample LMAR-5 is a sandstone from strata of the upper part of the El Toqui Formation at the Chile Chico area. It yielded a maximum depositional age of ~127 + 2/−4 Ma (n = 6 of 104) with a prominent Jurassic (188 Ma) age peak. There are no Lower Jurassic rocks in the Central Patagonian Andes. Rocks of that age crop out in regions of the extra-Andean domain (see Pankhurst et al., 2000), but are located too far to the northeast to constitute a reliable source area. The 188 Ma zircons could derive from the Upper Jurassic–Berriasian (152–142 Ma) Ibáñez Formation or the 153 Ma Río Blanco granite, which are the oldest Jurassic rocks in the area (De la Cruz and Suárez, 2008). This could indicate that some of these units are older than currently considered but this notion should be confirmed by further studies.

We collected two samples from sandstones of the Ligorio Márquez Formation in the Chile Chico area. Sample LMAR-2, from the lower part of the unit, yielded a maximum depositional age of ~75 + 1/−2 Ma (n = 4 of 118), with major peaks at 82 Ma, 117 Ma

Table 1
Summary of calculated U-Pb zircon ages and other age groups.

Sample	Formation	Lithology	Section	Calculated age $^{206}Pb/^{238}U$ (Ma) (2σ)	Other age peaks (Ma)
PCD15-6	El Toqui	Tuff	Pampa Castillo	133.9 ± 1.9	
LMAR-5	El Toqui	Sandstone	Ligorio Márquez	126.5 + 2.3/−4.2	188
LMAR-2	Ligorio Márquez	Sandstone	Ligorio Márquez	74.7 + 0.8/−1.9	82, 117, 185
LMD15-1	Ligorio Márquez	Sandstone	Ligorio Márquez	79.5 + 4.0/−3.9	115, 143, 177
PGD15-2	San José	Tuff	Pampa Guadal	38.8 ± 0.6	107, 137
PCA-6	San José	Tuff	Pampa Castillo	40.6 ± 0.5	131
MGUADAL-2	San José	Pumice rich sandy conglomerate	Pampa Castillo	28.3 + 0.5/−0.4	
PCA4	Guadal	Sandstone	Pampa Castillo	23.4 ± 1.0	82, 115
MGUADAL-3	Guadal	Sandstone	Pampa Castillo	19.8 + 0.3/−0.4	34, 125

and 185 Ma. Sample LMD15-1, from the upper part of the formation, yielded a maximum depositional age of ~80 ± 4.0 Ma ($n = 6$ of 55), and major age populations at 115 Ma, 143 Ma, and 177 Ma. The 185 Ma, 177 Ma, and 143 Ma peaks could derive from the Ibáñez Formation, which crops out to the east and west of the Ligorio Márquez Formation, or the Río Blanco granite, which is exposed in a small area west of this unit (see previous). The 117 Ma and 115 Ma zircons likely derive from the Aptian Divisadero Formation, which underlies the Ligorio Márquez Formation. The 82 Ma, 80 Ma, and 75 Ma groups are probably derived from Upper Cretaceous subvolcanic rocks that crop out to the southwest of the Chile Chico area (see De la Cruz et al., 2004; De la Cruz and Suárez, 2008). These data do not indicate a precise provenance area for the Ligorio Márquez Formation but the location of some of the possible source rocks (the Río Blanco granite and the Upper Cretaceous subvolcanic rocks) suggests a western origin.

We obtained three samples from the San José Formation at Meseta Guadal. Sample PGD15-2 is a tuff from the base of this unit at the Pampa Guadal section and yielded an age of ~39 ± 0.6 Ma ($n = 33$ of 52), plus two peaks of 107 Ma and 137 Ma. Sample PCA6 is also a tuff from the middle to upper part of the San José Formation at the Pampa Castillo section that yielded an age of ~41 ± 0.5 Ma ($n = 87$ of 94) and a small group peak at 131 Ma. Sample MGUADAL-2 is a sandy conglomerate with abundant pumice clasts from the upper part of the San José Formation in the Pampa Castillo section that yielded a maximum age of ~28 ± 0.5 Ma ($n = 69$ of 75) and six individual ages that range from 38 Ma to 614 Ma. The 137 Ma and 131 Ma zircons likely derive from the Tithonian-Valanginian El Toqui Formation, which underlies the San José Formation and crops out to the SE of this unit. The 107 Ma group could derive from plutonic rocks that crop out to the east, north, and south of Meseta Guadal. The 41 Ma and 39 Ma populations could be related to volcanic and subvolcanic rocks that crop out principally to the east and also to the south of Meseta Guadal (either from contemporaneous explosive volcanism or erosion of these rocks). The youngest 28 Ma zircons could be related to basaltic subvolcanic rocks that crop out to the south of Meseta Guadal (see De la Cruz et al., 2004; De La Cruz and Suárez, 2006). Based on the location of some of the possible source rocks (e.g., El Toqui Formation or the Eocene subvolcanic rocks) the provenance area for the San José Formation sediments appears to have been located east of Meseta Guadal.

Finally, we collected two samples from the Guadal Formation at the Pampa Castillo section. Sample PCA4 is a sandstone from the base of this unit that yielded a maximum late Oligocene–early Miocene age (~23 ± 1 Ma, $n = 5$ of 106) and peak ages at 82 Ma and 115 Ma. Sample MGUADAL-3 is a sandstone from the top of the Guadal Formation that yielded an early Miocene maximum depositional age (~20 ± 0.4 Ma, $n = 25$ of 111) with two important age peaks at 34 Ma and 125 Ma. The oldest peak of 125 Ma could derive from the Patagonian batholith to the west of Meseta Guadal or the Hauterivian-Atpian Apeleg Formation to the south and to the east. The 115 Ma zircons could derive from plutonic rocks to the north or from the Divisadero Formation to the east. The 82 Ma peaks from plutonic rocks to the southwest. The 34 Ma group could derive from volcanic and subvolcanic rocks that crop out principally to the east and secondarily to the south of Meseta Guadal, or this group could be derived from the erosion of the San José Formation strata. The 23 Ma and 20 Ma groups could be related to basaltic and dacitic subvolcanic rocks that crop out to the south and east of Meseta Guadal. As with the San José Formation, the location of some of the possible source rocks (Divisadero Formation, Eocene and Oligo-Miocene volcanic and subvolcanic rocks) suggests an eastern origin for the Guadal Formation sediments.

5. $^{40}Ar/^{39}Ar$ geochronology

In order to determine the age of the BIMCC Formation we dated a basalt from the base of this unit at Mina Ligorio Márquez with the $^{40}Ar/^{39}Ar$ whole rock method.

5.1. Analytical method

$^{40}Ar/^{39}Ar$ geochronology was performed at the USGS Argon Geochronology facility in Denver, CO, USA. A whole rock basalt sample was crushed, and 1.0–1.7 mm diameter pieces were washed, handpicked for analysis under a binocular microscope, and loaded into Al discs together with the neutron flux monitor, Fish Canyon sanidine (FCs). Discs were wrapped in Al foil and sealed under vacuum in a quartz glass vial, which was wrapped in Cd foil. The package was irradiated for 20 h at the 1 MW USGS TRIGA reactor. Samples and standards were analyzed on a Thermo Scientific ARGUS VI mass spectrometer at the USGS Argon Geochronology Laboratory in Denver, Colorado, on 23 Dec 2016. Gas release was accomplished by heating using a Photon Machines 50 W CO_2 laser. Noble gas purification was achieved with SAES getters and a cryogenic trap. Argon isotopes were detected using four Faraday detectors (^{40}Ar, ^{39}Ar, ^{38}Ar, and ^{37}Ar) and one ion counter (^{36}Ar), and measured abundances were determined using the MassSpec software package (authored by Al Deino, Berkeley Geochronology Center). Full argon isotope data, corrected for baselines, backgrounds, mass discrimination, detector intercalibration, nucleogenic interferences, and decay, are provided in Table DR2. Background measurements were run every two analyses. Backgrounds were fit with a weighted mean ± 1 standard deviation. Discrimination and $^{40}Ar/^{36}Ar$ detector intercalibration factors were determined via a long-term average of measurements of three air

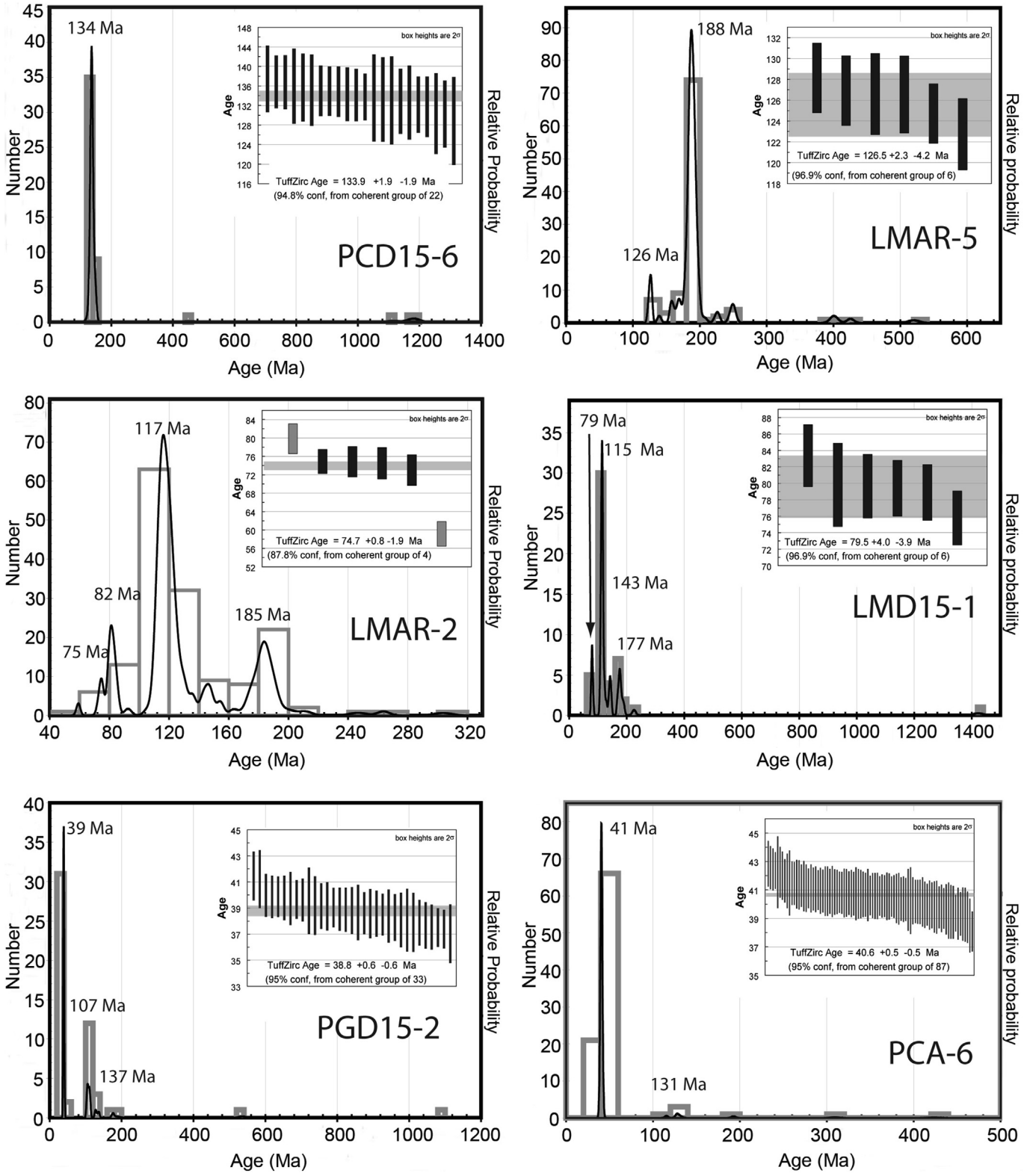

Figure 8. U-Pb ages and probability density plots for detrital zircon samples from the El Toqui, Ligorio Márquez, and San José formations.

pipettes approximately twice per day, using the atmospheric $^{40}Ar/^{36}Ar$ value of Lee et al. (2006). Samples were co-irradiated with FCs and ages were calculated using an age for FCs of 28.201 ± 0.023 (1σ) (Kuiper et al., 2008). Decay constants used were those of Min et al. (2000) for ^{40}K, and Stoenner et al. (1965) for ^{37}Ar and ^{39}Ar. Nuclear interference production ratios for $(^{40}Ar/^{39}Ar)K$, $(^{36}Ar/^{37}Ar)Ca$, and $(^{39}Ar/^{37}Ar)Ca$ are based on measurements of potassium-rich glass and CaF_2 co-irradiated with samples; other interferences were corrected using values for Cd-shielded fission-spectrum neutrons from Renne et al. (2005).

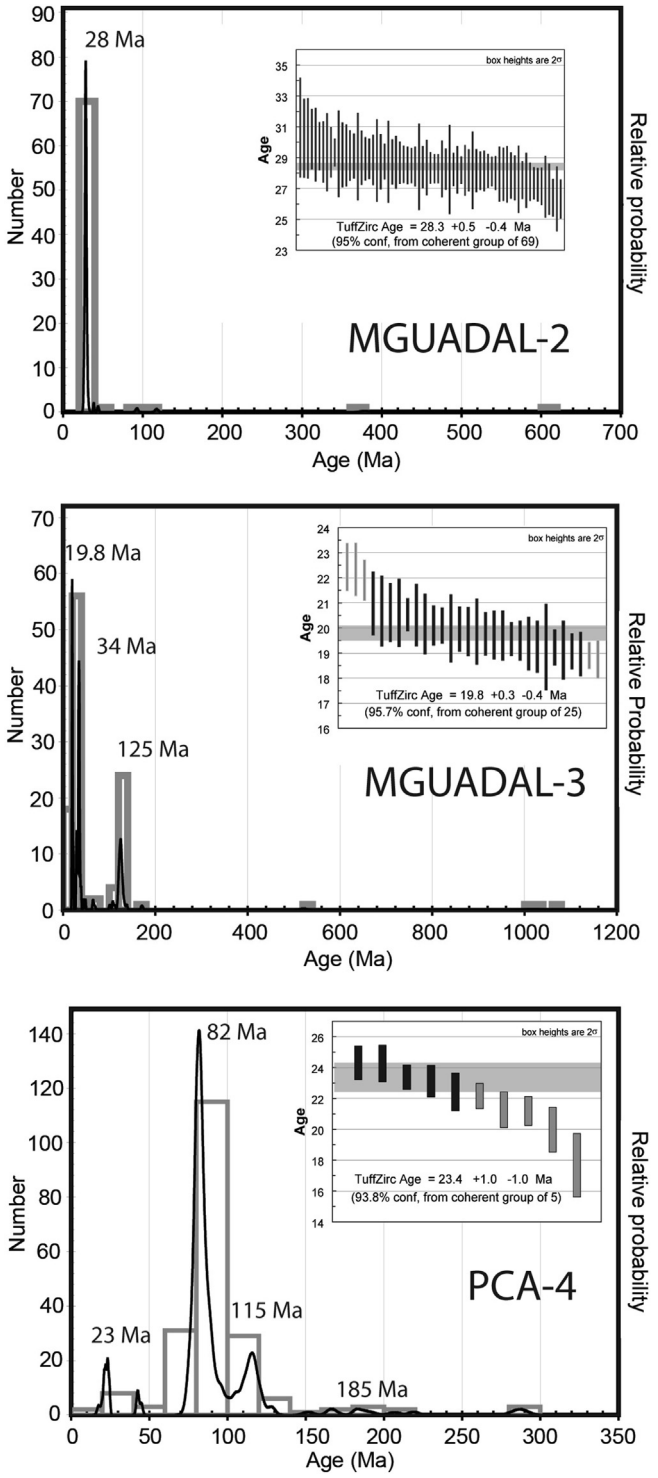

Figure 9. U-Pb ages and probability density plots for detrital zircon samples from the San José and Guadal formations.

5.2. Results

We sampled fresh basalt (sample 15LJ70) from a flow at the base of the BIMCC Formation overlying an exposed section of the Ligorio Márquez Formation near the Mina Ligorio Márquez locality (46.8°S, 71.8°W). This locality (Fig. 2) lies southwest of Chile Chico and was described by Suárez et al. (2000). This exposure of the Ligorio Márquez Formation is Paleocene–Eocene based on leaf fossils (Suárez et al., 2000) and detrital zircons (Breen et al., 2015). The resulting whole-rock $^{40}Ar/^{39}Ar$ age for the overlying basalt is 53.4 ± 0.2 Ma (MSWD = 0.87) (Fig. 10). The age spectrum shows an excess of Ar (Fig. 10A), which leads to a somewhat non-atmospheric intercept (Fig. 10B). However, the age is determined by a series of very radiogenic steps, making it insensitive to the excess Ar.

6. Petrography and geochemistry of the San José formation volcanic rocks

6.1. Petrography

Pyroclastic rocks and lava flows are interbedded with sedimentary strata of the San José Formation (Figs. 5 and 6). In order to understand the tectonic setting of this unit, we carried out petrographic and geochemical analyses. Significantly, this is the first chemical analysis for the volcanic rocks of the San José Formation. Volcanic rocks also occur in the BIMCC and BSMCC formations. We studied the petrography of two samples from the BIMCC Formation; geochemical analyses on both basalt units were previously performed by Espinoza et al. (2005).

Most of the volcanic rocks in the San José Formation comprise dark-greyish pyroclastic rocks, classified as tuffs and lapillitic tuffs. Samples are mainly composed of a fine-grained matrix (>80%), with

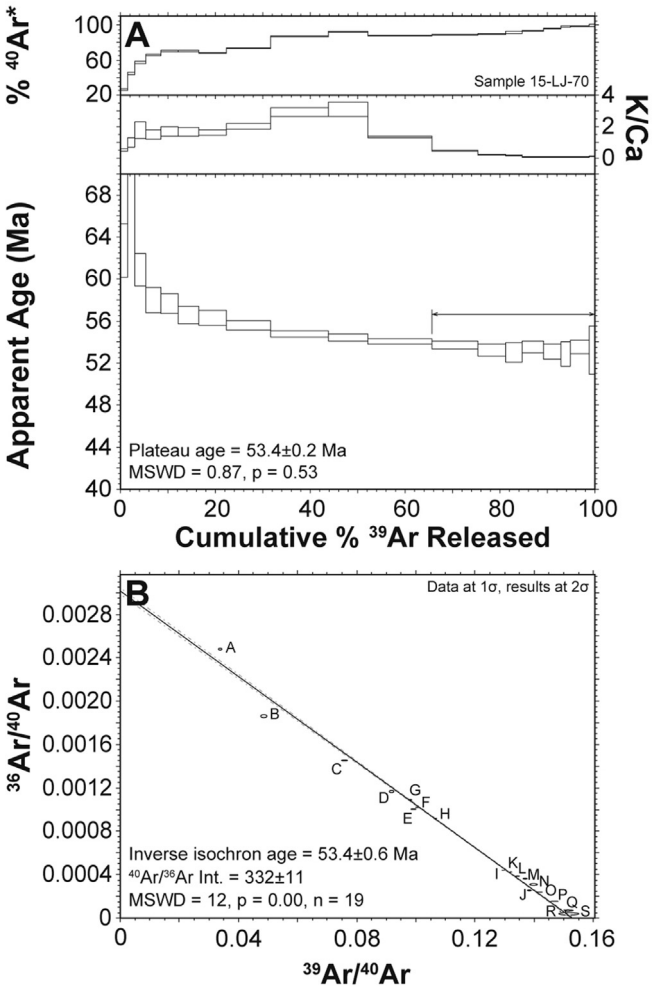

Figure 10. $^{40}Ar/^{39}Ar$ results for BIMCC Formation sample 15LJ70 from the Ligorio Márquez section, including the (A) argon release spectra and (B) inverse isochron.

crystal and lithic fragments occasionally visible in hand specimen. Lithic fragments are subangular, up to 2–3 mm in size, and correspond to very-fine grained or aphanitic lithologies. Lavas are scarce and include both dark rocks with both aphanitic and porphyritic textures, the latter with 2–3 mm plagioclase phenocrysts.

In the Pampa Castillo section, interbedded volcanic rocks are located in the upper part of the San José Formation (Fig. 5). They are typically crystal-rich (60%) tuffs composed mainly of quartz, with common embedded rims, and subordinate plagioclase and mafic phases, the latter replaced by opaque minerals (Fig. 6K). The matrix consists of volcanic ash and palagonitized vitreous fragments, with occasional intense carbonate replacement.

Crystalline dacitic to rhyolitic tuffs are also interbedded in the lower part of the San José Formation at the Pampa Guadal section (Fig. 5). Most of the samples share the same general petrographic features: crystal content (50%) includes quartz, plagioclase, and minor opaque minerals fragments. Pumice fragments (30%) are moderately altered to brownish clays, while lithic fragments (20%) are quartzite or polycrystalline quartz, with some samples also including intermediate volcanic rocks, mostly with plagioclase microlites. The matrix in all of the samples is vitreous, with moderate to intense clay alteration, and also includes fine-grained palagonitized vitreous fragments. Despite the penetrative alteration observed in the matrix, primary textures and mineral associations of the tuffs are preserved, although samples at the top of the profile are intensely replaced by oxides. A basaltic lava flow is interbedded near the top of San José Formation in the Pampa Guadal profile. Petrography shows it is a porphyritic rock with 15% of olivine phenocrysts within an intergranular groundmass (Fig. 6L). Olivine phenocrysts are 1–1.5 cm subhedral grains with moderate bowlingite alteration at the border. The groundmass is comprised mostly of plagioclase microlites (50%) and fine-grained brownish clinopyroxene (40%), with subordinate opaque minerals (10%).

Pyroclastic rocks in the upper part of the San José Formation at the Las Dunas section consist mainly of vitreous to crystalline dacitic tuffs, interbedded at the upper part of the section. Pyroclasts (60%) consist of up to 50% of well-preserved pumice fragments and 40% of crystals, mainly plagioclase, and minor quartz and opaque minerals. Subordinate subrounded pyroclastic lithoclasts (10%) are also present. The matrix (40%) is composed of brownish volcanic ash, which shows intense clay alteration and fine-grained volcanic shards with smectite replacement.

Volcanic rocks at the upper part of the San José Formation at the Las Horquetas section correspond to crystalline trachytic to rhyolitic tuffs and lapillitic tuffs. Pyroclasts (50%) include 60% of crystals, 30% of volcanic lithoclasts and 10% of clay-altered pumice fragments within a clay-rich matrix. Crystal content is mainly K-feldspar, minor quartz, plagioclase and opaque minerals. Intermediate volcanic lithoclasts are characterized by porphyritic textures. Near the top of the section, interbedded volcanic rocks comprise a fine- to intermediate-grained mafic andesite. It shows porphyritic texture under the microscope, with phenocrysts (10%) mostly of green to brown pleochroic amphiboles forming large subhedral prisms (2 mm) and minor subhedral clinopyroxene (1 mm). The groundmass consists of a felty assemblage (90%), mostly composed of plagioclase and amphibole (~0.5 mm) and minor clinopyroxene (~0.3 mm). The primary mineral association is mostly unaltered; however, ferromagnesian secondary phases and clay association are found interstitially within the groundmass. The porphyritic texture with a fine to intermediate grain size within the groundmass suggests a subvolcanic emplacement for this rock, consistent with the interpretation of Flint et al. (1994).

We studied the petrography of two samples from the basal part of the BIMCC Formation in the Chile Chico area. They are dark, fine-grained basalts, which show a porphyritic texture under the microscope with 10% to 15% of 2 mm olivine phenocrysts within a plagioclase (1.5 mm) and clinopyroxene-rich (0.3 mm) groundmass (Fig. 6F). Euhedral to subhedral olivines show moderate to intense bowlingite and serpentine alteration from the rim to the core of the crystals and within fractures. Subhedral plagioclase microlites and reddish pyroxene are relatively fresh. Secondary very fine-grained ferromagnesian phases are interstitially distributed within the groundmass and fractures, as well as minor secondary carbonates.

6.2. Geochemistry

We selected 7 representative volcanic rocks within the San José Formation to carry out geochemical analyses. Given the variable degree of alteration, we chose the fresher samples and removed lithic fragments in the more lithic-rich ones. Samples LFOS-2, PGD15-3, PGD15-7 and PGD15-9 are tuffs from the lower part of the Pampa Guadal section while sample LFOS-4 (Fig. 6L) is a basalt from the upper part of this profile (Fig. 5). Sample LDD15-1 is a tuff that lies at the upper part of the Las Dunas section, and sample LHD15-4 corresponds to the mafic andesitic sill in the upper part of the Las Horquetas section.

Samples for geochemical analyses were prepared and analyzed at the Activation Laboratories of Ancaster, Ontario, Canada (www.actlabs.com). Rock samples were mixed with a flux of lithium metaborate and lithium tetraborate and fused in an induction furnace. Major and trace elements were analyzed by fusion inductively coupled plasma mass spectrometry (ICP-MS). Results and detection limits are presented in Table DR3.

Silica contents range from 68.92 wt.% to 74.28 wt.% for the volcanic samples located at the base of the San José Formation (LFOS-2, PGD15-1, PGD15-7 and PGD15-9). Rock samples from the upper part of this unit show lower silica content between 57.3 wt.% and 61.51 wt.% (LFOS-4 and LDD15-1). Sample LHD15-4, interpreted to be a sill, has 48.41 wt.% SiO_2. The post-emplacement alkali loss and pervasive alteration precludes the use of rock classification schemes and analyses based on major elements. However, trace element behavior shows no signs of alteration during secondary processes, as it is not correlated with LOI values.

Primitive mantle-normalized trace element abundances show patterns that vary according to silica content (Fig. 11A). Samples from the lower part of the San José Formation (>63 wt.% SiO_2) show enrichment in large-ion lithophile elements (LILE) relative to high field strength elements (HFSE) and rare earth elements (REE). These patterns resemble an arc signature, with a characteristic trough in Nb. Negative anomalies in Rb and K in these silica-rich samples are explained by K-feldspar fractionation. Samples from the upper part of the San José Formation (52–63 wt.% SiO_2) reflect a clearer arc signature, as they show higher LILE enrichment and more pronounced negative Nb and Ti anomalies. The mafic andesitic sill (sample LHD15-4, <52 wt.% SiO_2) has a smoother pattern with a less arc-like signature. Chondrite-normalized REE diagrams are similar for most of the samples (Fig. 11B). The higher contents of the light REE (LREE) compared to the heavy ones (HREE), together with the relatively concave patterns, indicate pyroxene and amphibole fractionation. Samples with >63 wt.% SiO_2 have patterns with relatively steeper slopes (La/Yb = 8.61–5.05) than samples between 52 wt.% and 63 wt.% SiO_2 (La/Yb = 4.36–3.50), and samples with <52 wt.% SiO_2 (La/Yb = 5.98).

7. Discussion

7.1. Age and correlations

Our geochronologic data, in combination with those obtained in recent contributions (Breen et al., 2015; Suárez et al., 2015) indicate

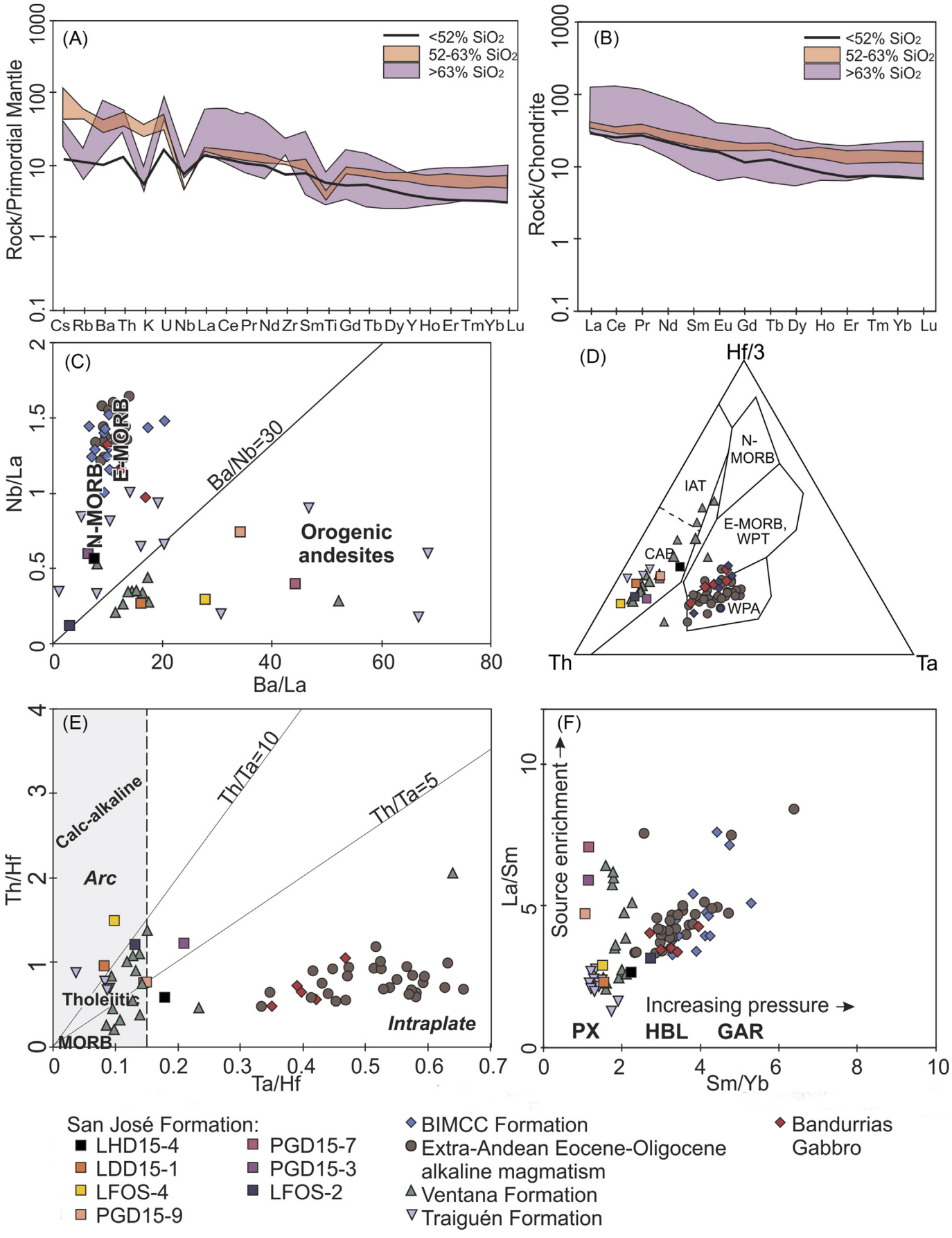
(A)
<52% SiO2
52-63% SiO2
>63% SiO2
Rock/Primordial Mantle
Cs Rb Ba Th K U Nb La Ce Pr Nd Zr Sm Ti Gd Tb Dy Y Ho Er Tm Yb Lu
(B)
Rock/Chondrite
La Ce Pr Nd Sm Eu Gd Tb Dy Ho Er Tm Yb Lu
(C)
Nb/La
Ba/La
Ba/Nb=30
N-MORB
E-MORB
Orogenic andesites
(D)
Hf/3
Th
Ta
N-MORB
IAT
E-MORB, WPT
CAB
WPA
(E)
Th/Hf
Ta/Hf
Calc-alkaline
Arc
Tholeiitic
MORB
Th/Ta=10
Th/Ta=5
Intraplate
(F)
La/Sm
Sm/Yb
Source enrichment
Increasing pressure
PX
HBL
GAR
San José Formation:
LHD15-4
LDD15-1
LFOS-4
PGD15-9
PGD15-7
PGD15-3
LFOS-2
BIMCC Formation
Extra-Andean Eocene-Oligocene alkaline magmatism
Ventana Formation
Traiguén Formation
Bandurrias Gabbro

the presence of a nearly complete Cenozoic record in the Central Patagonian Andes at ~47°S (Figs. 4 and 8–10). This refutes previous interpretations of a hiatus between the middle Eocene and late Oligocene (De La Cruz and Suárez, 2006). Below, we discuss the age of the different Cenozoic formations that crop out in the study area and correlate them with coeval units in the forearc, Andean Cordillera, and retroarc of this region.

Although our work focuses on the Cenozoic successions, we obtained two U-Pb ages from strata of underlying non-fossiliferous Cretaceous units in order to test their previously reported Mesozoic age (Fig. 8, Table 1). At Meseta Guadal, we dated a tuff of the upper part of the El Toqui Formation and obtained an U-Pb age of ~134 ± 2 Ma (sample PCD15-6). This age is roughly similar to the 139 ± 3 Ma K/Ar age obtained by De La Cruz and Suárez (2006) for the same unit in a nearby locality. At Mina Ligorio Márquez, we dated a sandstone from the upper part of the El Toqui Formation and obtained an U-Pb maximum depositional age of ~127 + 2/−4 Ma (sample LMAR-5). Suárez et al. (2000) obtained a similar age of 128 ± 3 Ma in a nearby locality.

We obtained U-Pb ages of ~75 + 1/−2 Ma and ~80 ± 4 Ma from detrital zircons of two sandstone beds from the lower (sample LMAR-2) and upper (LMD15-1) parts of the Ligorio Márquez Formation, respectively (Fig. 8, Table 1). Suárez et al. (2015) employed the same method and also obtained a Maastrichtian age for the youngest peak of detrital zircons as well as two individual zircon grains of 56–61 Ma respectively that are not statistically significant. Breen et al. (2015) also dated detrital zircons from several sandstone strata of the Ligorio Márquez Formation and obtained dates between 62 Ma and 50 Ma (early Paleocene–early Eocene). The youngest peak (3 grains) from a sandstone bed <3 m below the top of the section yielded an age of ~52 ± 3 Ma (Breen et al., 2015). Because detrital zircons provide maximum depositional ages, and the ~52 Ma age of Breen et al. (2015) is younger than those obtained by us and Suárez et al. (2015), it must be closer to the age of deposition. The ~52 Ma U-Pb age is also in agreement with the late Paleocene–early Eocene age proposed by Suárez et al. (2000) based on the study of fossil flora from the Ligorio Márquez Formation. According to these data, this unit can be temporally correlated with the lower–middle part of the Río Chico Group, a Paleocene–Eocene fluvial unit that crops out in the extra-Andean region in central Patagonia and has been recently dated in ~63 Ma to 42 Ma (Clyde et al., 2014; Krause et al., 2017) (Fig. 4).

We obtained a $^{40}Ar/^{39}Ar$ age of 53.4 ± 0.2 Ma (sample 15LJ70; Fig. 10) for a basalt at the base of the BIMCC Formation near the Mina Ligorio Márquez locality. Previous radiometric data from this unit include more than 30 K/Ar ages (mostly whole rock) indicating dates between ~57 Ma and 34 Ma (Charrier et al., 1979; Baker et al., 1981; Flynn et al., 2002; Espinoza et al., 2005; Yabe et al., 2006; De la Cruz and Suárez, 2008). Of these, three ages have been reported for the base of the BIMCC Formation at the Mina Ligorio Marquéz, two of 47.5 ± 1.1 Ma and 47.7 ± 1.1 Ma (K/Ar, plagioclase) by Yabe et al. (2006) and one of 41.6 ± 1.4 Ma (K/Ar, whole rock) by De la Cruz and Suárez (2008). It is evident that the ages obtained by these authors and our $^{40}Ar/^{39}Ar$ age differ considerably. Also noticeable is the fact that, while most radiometric ages from the BIMCC Formation range between ~55 Ma and 40 Ma, some of them are substantially younger such as those of 34.9 Ma, 34.1 Ma, and 33.5 Ma obtained by Flynn et al. (2002). In fact, these ages overlap with those assigned by us to the San José Formation. It is possible that part of the volcanic rocks assigned to the BIMCC Formation correspond to a younger unit. However, as most of these dates were obtained through the whole rock K/Ar method, it is also plausible that at least some of them are erroneous since the basalts of the BIMCC are altered (Espinoza et al., 2005), as the K/Ar system is susceptible to modification of both parent and daughter isotopes. In this regard, our 53.4 ± 0.2 Ma $^{40}Ar/^{39}Ar$ date for the base of this unit is probably more reliable. This early Eocene age is statistically identical to the ~52 ± 3 Ma U-Pb maximum detrital zircon age obtained by Breen et al. (2015) for the top of the Ligorio Márquez Formation, indicating that deposition of these units was probably transitional or with a minimal hiatus. Despite the issues with the K/Ar system, the spread of K/Ar ages of the BIMCC Formation (~55 Ma and 40 Ma) appears to correlate with K/Ar ages of the ~57–45 Ma Posadas Basalt (Baker et al., 1981; Kay et al., 2002) and with the ~59–46 Ma Balmaceda Basalts (Baker et al., 1981; De la Cruz et al., 2003), which are located east and north of the Chile Chico area, respectively.

We obtained U-Pb ages of ~39 ± 0.6 Ma, ~41 ± 0.5 Ma, and ~28 ± 0.5 Ma for the San José Formation (samples PGD15-2, PCA-6, and MGUADAL-2; Figs. 8 and 9). The oldest samples are tuffs (PGD15-2 and PCA-6) and their ages are considered as to be depositional (see section 4.2). Sample MGUADAL-2 is a conglomerate and therefore its age is considered maximum. However, the presence of abundant pumice material in this sample indicates that deposition was likely contemporaneous with nearby volcanism, which implies that the younger zircon ages are probably very close to the age of deposition. This is supported by the fact that most of the zircon ages from the analyzed samples correspond to the younger peaks. However, there is a discrepancy between the ~39 ± 0.6 Ma age of sample PGD 15-2 and the ~41 ± 0.5 Ma age of sample MGUADAL-2, because the first was obtained from the basal part of the San José Formation at Pampa Guadal and the second is from the upper part of this unit at Pampa Castillo (Fig. 5). This implies that the lower part of the latter section is older than the base of the Pampa Guadal section. Alternatively, the lower part of the San José Formation at Pampa Castillo might correspond to the Ligorio Márquez Formation as proposed by De La Cruz and Suárez (2006), but neither we nor these authors found any evidence for an unconformity within the fluvial succession in this locality. On the other hand, sample MGUADAL-2 was not obtained from the top of the San José Formation, which implies that the upper part of this unit must be younger than ~28 ± 0.5 Ma and could be transitional with the overlying late Oligocene–early Miocene Guadal Formation. In support of this idea, the coal bed observed in the uppermost part of the San José Formation at Pampa Guadal (see section 3.3) could have formed as a consequence of the initial stages of the marine transgression that deposited the Guadal Formation.

The ~40 Ma to <28 Ma age (middle Eocene–late Oligocene) for the San José Formation is one of the most important contributions of this work. This unit had previously been considered upper Paleocene–lower Eocene based on its fossil macroflora (De La Cruz and Suárez, 2006), which should be restudied at the light of the new findings. This revised age means that the fluvial strata of the San José Formation cannot be correlated with those of the Ligorio Márquez Formation as proposed by Ray (1996). In this new context,

Figure 11. (A) Primitive mantle normalized multi-element diagram (Sun and McDonough, 1989). (B) Chondrite-normalized REE diagram (Nakamura, 1974). (C) Nb/La vs. Ba/La ratios, showing San José Formation volcanic rocks that most closely resemble orogenic andesites compositions. (D) Ta–Th–Hf/3 discrimination diagram, with San José Formation samples falling in the field of destructive plate-margin basalts and differentiates (Wood, 1980). (E) Th/Hf vs. Ta/Hf diagram, showing mostly tholeiitic arc-like sources for the San José Formation volcanic rocks. (F) La/Sm vs. Sm/Yb ratios. Studied rocks show low La/Sm and Sm/Yb, suggesting magmas were in equilibrium within pyroxene stability field. Our data is compared with the Eocene BIMCC Formation (Espinoza et al., 2005), Eocene–Oligocene alkaline magmatism (Kay et al., 2002; Bruni et al., 2008; Menegatti et al., 2014), Ventana Formation (Rapela et al., 1988; Kay et al., 2007; Fernández Paz et al., 2018), Oligocene Bandurrias Gabbro (Morata et al., 2005), and Traiguén Formation (Encinas et al., 2016a,b).

the San José Formation correlates with volcanic and subvolcanic rocks between 40 Ma and 24 Ma exposed in small outcrops in the Central Patagonian Andes (De la Cruz et al., 2004; Morata et al., 2005; De La Cruz and Suárez, 2006, 2008; De la Cruz and Cortés, 2011; Gianni et al., 2017a,b). In the extra-Andean region it partially correlates with the 41.7 Ma to 18.8 Ma Sarmiento Formation (Ré et al., 2010) and with the late Eocene to early Oligocene marine strata of the El Huemul Formation (Paredes et al., 2015). To the west, it is partially coeval with the Puerto Good sequence in the Golfo de Penas (Forsythe and Nelson, 1985), and with a 32 Ma age for a volcanic breccia of the Mitahues Island, which likely belongs to the basal part of the Traiguén Formation (Encinas et al., 2016a) (Fig. 4).

We U-Pb dated detrital zircons from two sandstone beds of the Guadal Formation at the Pampa Castillo section and obtained maximum depositional ages of ~23 ± 1.0 Ma (sample PCA4) for the base of this unit and of ~20 ± 0.4 Ma (sample MGUADAL-3) for the upper part (Fig. 9). Suárez et al. (2015) obtained an additional U-Pb age of ~19 Ma from a sandstone bed of the Guadal Formation in the same area. Accordingly, Frassinetti and Covacevich (1999) interpreted the invertebrate fauna of the Guadal Formation as late Oligocene–early Miocene based on a stratigraphic correlation with the Monte León Formation of Argentina. The Guadal Formation can be also correlated with the 20.3 Ma to 18.1 Ma El Chacay Formation, which crops out in the Lago Posadas-Meseta Belgrano region (47°30′S) and corresponds to the southern extension of the Guadal Formation in Argentina (Cuitiño et al., 2015). To the west, the Guadal Formation partly correlates with the ~26–23 Ma Traiguén Formation (Encinas et al., 2016a), and with deep-marine strata of probable late Oligocene–early Miocene age in the Golfo de Penas (lower part of the Grupo Chaicayan sequence; see Forsythe and Nelson, 1985; Encinas et al., 2015) (Fig. 4).

The vertebrate fauna of the Pampa Castillo Formation was assigned to the early Miocene Santacrucian SALMA by Flynn et al. (2002) and Bostelmann and Buldrini (2012). Suárez et al. (2015) obtained a U-Pb (SHRIMP) age of ~18 Ma from a tuff of the Santa Cruz Formation presumably sampled at the Pampa Castillo section. ~19 Ma to 12 Ma fluvial synorogenic deposits of the Santa Cruz Formation and younger units crop out extensively in the Central and Southern Patagonian Andes between the Andean Cordillera and the Atlantic coast (De Iuliis et al., 2008; Rivas et al., 2015; Suárez et al., 2015; Cuitiño et al., 2016; Encinas et al., 2016b) (Fig. 4). To the west, the middle-upper Miocene upper unit of the marine Grupo Chaicayán sequence (Forsythe and Nelson, 1985; Encinas et al., 2015) partly correlates with the Santa Cruz Formation and younger units.

Most published radiometric ages for the BSMCC Formation range between 12 Ma and 7 Ma (De la Cruz and Suárez, 2008, and references therein). Overlying this unit is the 5–3 Ma Basaltos Pico Sur Formation differentiated by De la Cruz and Suárez (2008) from the BSMCC Formation. The late middle to late Miocene BSMCC Formation can be correlated with the upper Miocene basalts of the Meseta Lago Buenos Aires Formation that crop out in western Argentina east of the Jeinemeni River (Ramos and Kay, 1992; Ecosteguy et al., 2003) (Fig. 4). It also correlates with other basaltic sequences of similar ages from central and southern Patagonia that have been grouped under the generic name of “Plateau Lavas” (Gorring et al., 1997).

7.2. Geochemical constraints on San José formation volcanic rocks and regional correlations

Volcanic rocks from the San José Formation have trace element ratios consistent with an arc-related signature (Fig. 11). Most of the samples show Ba/Nb values greater than 30 (Ba/Nb = 46.2–111.6), comparable to those of orogenic andesites (Gill, 1981). Exceptions to this behavior are shown by the silica-rich samples (LFOS-2 and PGD15-3) with lower Ba content due to K-feldspar fractionation, and sample LHD15-4, which corresponds to the mafic andesitic sill (Fig. 11C). The tectonic discriminant diagram shows that the San José Formation volcanic rocks consistently plot within the field of arc-related volcanism (Fig. 11D). Evidence for the arc-related behavior is also given by their Ta/Hf ratios <0.2, which together with Th/Hf values, suggest a tholeiitic composition. Samples in the upper part of the formation show a slight tendency towards a calc-alkaline source.

The U-Pb ages for the San José Formation and the stratigraphic location of the analyzed volcanic rocks within the profiles constrain the timing of this volcanism between the middle Eocene and the late Oligocene (~40–28 Ma). Overall, its geochemical characteristics suggest a genesis from arc-like tholeiitic to calc-alkaline sources, with input from slab-derived fluids. Trace element ratios, together with tectonic discrimination diagrams, indicate that the studied samples evolved in an arc setting. The San José Formation volcanic rocks show La/Yb (3.50–8.61) and Sm/Yb (1.07–2.74) indicative of magmas in equilibrium within the pyroxene stability field (Fig. 11F), which is consistent with low-pressure conditions expected in crust of normal thickness (~35 km) (e.g. Hildreth and Moorbath, 1988; Profeta et al., 2015). These geochemical features support the hypothesis that these magmas evolved under extensional or neutral, rather than contractional, conditions.

While the San Jose Formation volcanic rocks represent arc-related magmas evolving within low pressure conditions, coeval alkaline magmatism from both the Andean and extra-Andean regions shows intraplate-like E-MORB sources, developed within a garnet-spinel stability field, typical of OIB magmas (Kay et al., 2002; Espinoza et al., 2005; Morata et al., 2005; Bruni et al., 2008; Menegatti et al., 2014) (Fig. 11C–F). At a wider regional scale, arc-related activity during Mid-Eocene to Lower Miocene (37–20 Ma) includes mainly basaltic to andesitic lavas of the Ventana Formation exposed in the North Patagonian Andes (40°S–43°S) and the basaltic pillow-lavas of the Traiguen Formation in the western forearc (~45°30′S) (Rapela et al., 1988; Encinas et al., 2016a; Fernández Paz et al., 2018), all of which share an arc-like signature (Fig. 11). It is worth noting that the San José Formation volcanic rocks show low Sm/Yb ratios, like those characteristic of the Ventana and Traiguen formations volcanism, which are interpreted as developed during a period of progressive crustal thinning (Rapela et al., 1988; Bechis et al., 2014; Litvak et al., 2014; Encinas et al., 2016a; Fernández Paz et al., 2018). In summary, Eocene–upper Miocene volcanic rocks of the North and Central Patagonian Andes reflect geochemical signatures consistent with their magmatic evolution within a thin crust and extensional conditions.

7.3. Tectonic setting

The tectonic setting represented by the Cenozoic sedimentary and volcanic successions that crop out in the Central Patagonian Andes is not well understood (see Suárez and De La Cruz, 2000; De la Cruz et al., 2003). The geometric relationship between Mesozoic and Cenozoic stratified units in this area suggests that significant deformation did not occur during their deposition. The Paleocene–lower Eocene Ligorio Márquez Formation shows a subtle angular unconformity with Upper Jurassic–Lower Cretaceous strata of the El Toqui Formation and a disconformity with Lower Cretaceous strata of the Divisadero Formation. In a nearby area in western Argentina, the Ligorio Márquez Formation disconformably overlies the Lower–Upper Cretaceous Río Tarde Formation (Ecosteguy et al., 2003). The middle Eocene–lower

Oligocene San José Formation presents an angular unconformity (?) with Upper Jurassic–Lower Cretaceous rocks of the Ibáñez Formation and a paraconformity with Upper Jurassic–Lower Cretaceous of the El Toqui Formation. This suggests that compressive deformation between the early Late Cretaceous and the Paleocene was mild in this area.

Regarding tectonic deformation during the Cenozoic, the different units of this age that crop out in the study area show conformable or paraconformable contact relationships among them, which also suggests the absence of significant compressive deformation. Neither we nor previous workers have found structural evidence indicative of the tectonic setting in which the different Cenozoic Formations of the Central Patagonian Andes were deposited (see Suárez and De La Cruz, 2000; De la Cruz et al., 2003). The only exception is the synorogenic fluvial deposits of the early-middle Miocene Santa Cruz Formation and younger units (e.g., Lagabrielle et al., 2004; De La Cruz and Suárez, 2006). In the following, we discuss the tectonic setting for these Cenozoic units based on our data and those published by previous authors (Fig. 12). We also compare data from the Central Patagonian Andes with those from the forearc and the extra-Andean region, where structural information from seismic surveys is available.

Our geochronologic data indicate that the Ligorio Márquez Formation crops out exclusively in the Chile Chico area, west of the Jeinemeni Fault, and in a small area of Argentina east of the Jeinemeni river (Ecosteguy et al., 2003) (Fig. 3). We did not find any unequivocal evidence for the tectonic setting of this unit. The Ligorio Márquez Formation is coeval with the lower-middle part of the Río Chico Group that crops out in the extra-Andean region to the east (Clyde et al., 2014; Krause et al., 2017, and references therein) (Fig. 4). Based on seismic evidence, Navarrete et al. (2015) interpreted the basal levels of this group as synorogenic based on the wedging of its reflectors in the Río Senguer depocenter (46°S). However, we consider this evidence open to interpretation because thickness variation is minor (see Fig. 11 in Navarrete et al., 2015). If Navarrete et al. (2015) interpretation is correct, a compressional tectonic setting for the presumably coeval Ligorio Márquez Formation is plausible. In this context, paleocurrent analysis in this unit indicating a SSE direction could reflect surface uplift west of the Chile Chico area and deposition in a foreland basin (De la Cruz and Suárez, 2008). Our provenance analysis based on detrital zircons also favors a western source area. On the other hand, our geochronologic work indicates that deposition of the Ligorio Márquez and BIMCC formations appears to have been continuous. Thus, another option is that the tectonic setting of the Ligorio Márquez Formation was extensional, with the fluvial sediments of this unit deposited during the initial stages of basin subsidence that gave way later to the alkaline basalt volcanism of the BIMCC Formation (see below) (Fig. 12A). In favor of this notion, the Ligorio Márquez Formation shows a transition from braided to meandering fluvial systems, which is consistent with an increase of accommodation space during increasing extension.

The contact of the BIMCC Formation with the underlying Ligorio Márquez Formation is semi-covered, and its nature difficult to observe, but it has been defined as disconformable by De la Cruz and Suárez (2008). Given that the BIMCC Formation directly overlies Mesozoic units of the Ibáñez, El Toqui, and Divisadero formations at some localities, it is possible that an episode of uplift and erosion occurred between the deposition of the Ligorio Márquez and the BIMCC formations. Yet, geochronologic evidence suggests continuous, or almost continuous, deposition of these two units since U-Pb dating indicates a maximum depositional age of ~52 ± 3 Ma for the upper part of the Ligorio Márquez Formation and $^{40}Ar/^{39}Ar$ an age of 53.4 ± 0.2 Ma for the base of the BIMCC Formation. The overlap of these ages also opens up the possibility that the upper part of the Ligorio Marquez and the basal part of the BIMCC formations are contemporaneous.

The upper Paleocene to Eocene alkaline basalts of the BIMCC Formation were deposited in a backarc setting during a gap of arc volcanism (Ramos and Kay, 1992). They are relatively primitive, with a marked OIB-like signature (Espinoza et al., 2005). Results of partial melting-REE modeling indicate an origin by low degrees of partial melting from a primitive mantle source at depths within the garnet-spinel stability field (~65–70 km) (Espinoza et al., 2005). This suggests extension and crustal thinning in order to allow rapid ascent of uncontaminated magmas (Espinoza et al., 2005) (Fig. 12B). The origin of the BIMCC Formation and correlative units in the Patagonian Andes, such as the Balmaceda or Posadas Basalts, have been attributed to an asthenospheric upwelling linked to the opening of a slab window during the collision of the Aluk-Farallón spreading ridge with the Chilean trench (Ramos and Kay, 1992; Kay et al., 2002; Espinoza et al., 2005). On the other hand, Gianni et al. (2017a,b) observed syntectonic growth-strata in 43.9 Ma beds of the upper levels of the Río Chico Group in the extra Andean region (Fig. 4). This data is difficult to reconcile with the extensional setting suggested by geochemistry for the 55–40 Ma flood basalts of the Central Patagonian Andes and deserves further study.

The middle Eocene–Oligocene San José Formation crops out only in the Meseta Guadal area (Figs. 2 and 12C). It is not clear yet whether the upper part of the basaltic rocks assigned to the BIMCC Formation in the Chile Chico area is coeval with the San José Formation (see section 7.1). We did not observe structural evidence bearing on the tectonic setting for the San José Formation. However, our geochemical analysis of volcanic rocks from this unit suggests extensional or neutral tectonic conditions and an arc-related signature (see section 7.2), which could indicate an intra-arc setting. In support of an extensional tectonic regime, it is relevant to note that the San José Formation is not exposed east of the Meseta Guadal area, and paleocurrent analysis from this unit indicates a W to S direction (De La Cruz and Suárez, 2006). Accordingly, provenance analysis based on detrital zircons favors an eastern source area (see section 4.2). The age of the basal part of the San José Formation at the Pampa Castillo section appears to be older than that of the Pampa Guadal section and this unit is thicker in the first section than in the second one (Figs. 5 and 8), which indicates that basin subsidence probably progressed from east to west. These data suggest that the San José Formation was deposited in a half graben setting with an uplifted area limited by normal faults to the east (Fig. 12C). In contrast, continuous exposure and eastward paleocurrent directions for this unit would be expected in a foreland basin. Geologic evidence from other areas of the region also points out to an extensional regime during the middle Eocene–early Miocene. The 27 Ma Bandurrias Gabbro in the Andean Cordillera near Coyhaique was emplaced during an extensional or transtensional tectonic setting, according to its geochemical signature (Morata et al., 2005). The ~42 Ma to 19 Ma tuff deposits of the Sarmiento Formation and associated intraplate alkaline lava flows and intrusives in the extra Andean region have been related to extensional tectonics based on their geochemistry and seismic evidence (Bruni et al., 2008; Paredes et al., 2008, 2015; Ré et al., 2010; Gianni et al., 2015) (Fig. 4). In the same area, the late Eocene to early Oligocene marine strata of the El Huemul Formation also show seismic evidence for extensional tectonics (Paredes et al., 2015) (Fig. 4). The 26–23 pillow basalts and turbidites of the Traiguén Formation exposed in the limit between the forearc and the Andean range were also deposited in an extensional setting (Fig. 4), as indicated by the presence of synextensional growth strata and geochemical analysis (Encinas et al., 2016a,b). The only known coeval exception to the pattern of extensional tectonics is a ~40 Ma tuff unit from Meseta de Chalía (45°30′S) which shows

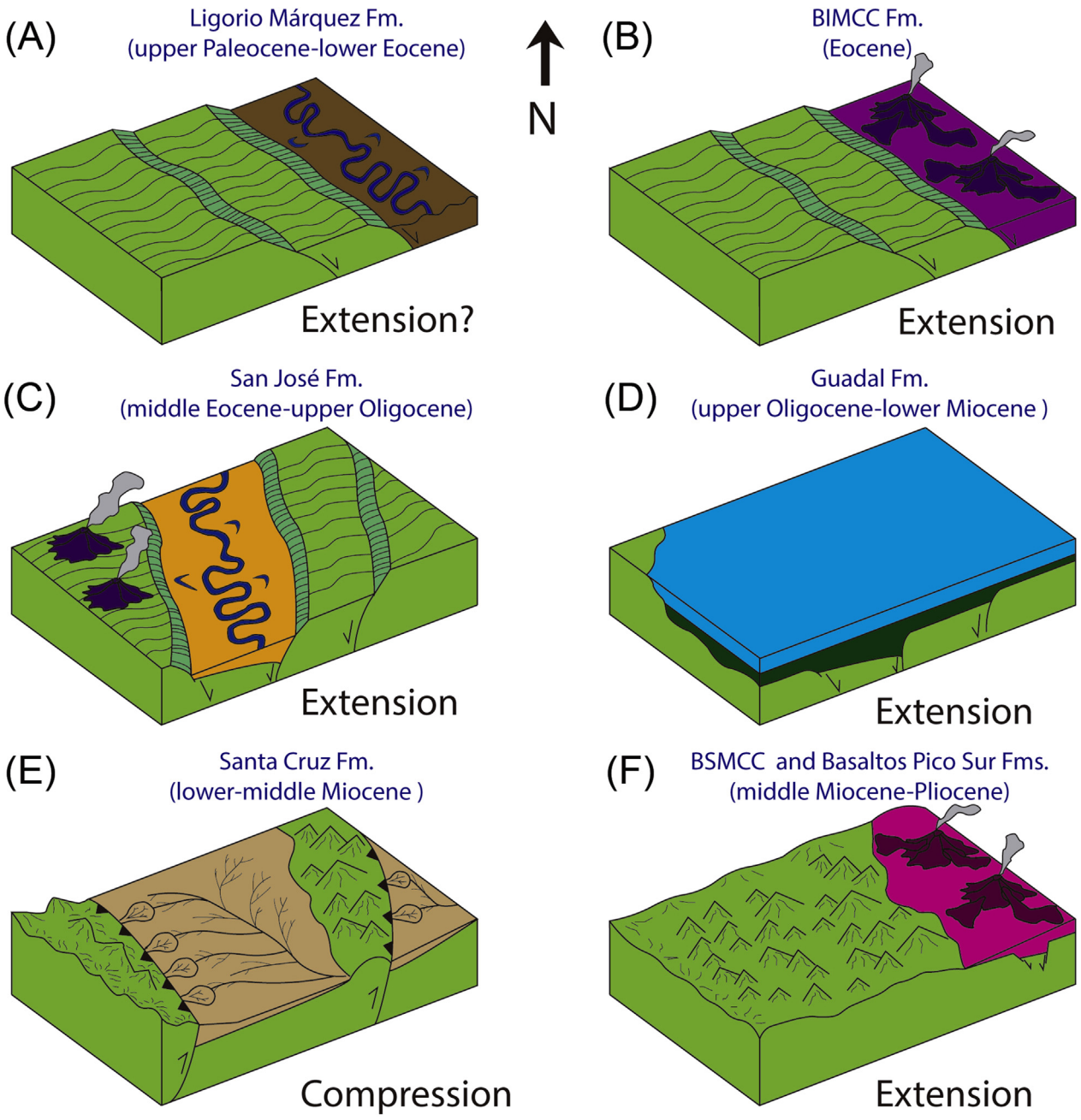

Figure 12. Paleoenvironmental cartoons showing the inferred tectonic phases that have impacted the Meseta Guadal (left) and Chile Chico (right) areas during the Cenozoic. We base our reconstructions on geochronologic, zircon provenance, stratigraphic, sedimentologic, paleocurrent analysis, and geochemical studies (see section 7.3 for a thorough explanation). Normal faults depicted in the diagrams are inferred. (A) Deposition of the fluvial strata of the upper Paleocene–lower Eocene Ligorio Márquez Formation in the Chile Chico area during a probable extensional phase. (B) Extrusion of the flood basalts of the Eocene BIMCC Formation in the Chile Chico area during an extensional phase related to the subduction of the Aluk-Farallon spreading ridge. (C) Deposition of the fluvial strata of the middle Eocene–upper Oligocene San José Formation in the Meseta Guadal area during an extensional phase. (D) Deposition of the upper Oligocene–lower Miocene marine deposits of the Guadal Formation in the Meseta Guadal and Chile Chico areas during a major marine transgression of Atlantic origin in a probable extensional setting. (E) Deposition of the fluvial synorogenic deposits of the lower–middle Miocene Santa Cruz Formation and younger units in the Meseta Guadal area and the Chile Chico area east of the Jeinemeni fault during a major compressive phase. (F) Extrusion of the flood basalts of the middle Miocene–Pliocene basaltic rocks of the BSMCC and Pico Sur formations in Chile and the Meseta Lago Buenos Aires and younger volcanic units in Argentina during an extensional phase related to the subduction of the Chile ridge.

growth strata that have been interpreted by Gianni et al. (2017a,b) as evidence of compressive tectonics. Encinas et al. (2016b) explained that it is difficult to discern whether these growth strata are related to extensional or compressive tectonics or to sedimentologic causes.

The late Oligocene–early Miocene marine strata of the Guadal Formation crop out in the Chile Chico and Meseta Guadal areas (Figs. 2 and 12D). At Chile Chico, this formation paraconformably (?) overlies the Paleocene–Eocene flood basalts of the BIMCC Formation, which indicates a hiatus between the deposition of these units. This suggests that after the extrusion of the basaltic sequence, the Chile Chico area became an area of positive relief before subsidence resumed in the late Oligocene–early Miocene, eventually allowing marine flooding. In the Meseta Guadal, on the

other hand, the ~28 Ma U-Pb maximum depositional age for the upper part of the San José Formation and the ~23 U-Pb maximum depositional age for the base of the late Oligocene–early Miocene Guadal Formation indicates that deposition of the fluvial and marine units was continuous or almost continuous in this area.

As noted before, there is not clear geologic evidence that indicates the tectonic context for the Guadal Formation. Provenance analysis based on detrital zircons favors an eastern source area (see previous), which agrees with previous paleogeographic reconstructions that propose an uplifted area to the east (e.g., Ramos, 1982; Cuitiño et al., 2015), although do not clarify whether there was an emergent area to the west and to the north as also proposed by these authors. The occurrence of late Oligocene–early Miocene marine deposits in the Meseta Guadal, at the axial part of the Central Patagonian Andes, indicates an attenuated crust of ≤33 km, according to conventional isostatic analyses (Introcaso et al., 2000). The geochemistry of the volcanic rocks from the underlying San José Formation is consistent with magmas evolving in a crust of ~35 km thick. In addition, the Guadal Formation shows lateral gradient in thickness, like the San José Formation at the Meseta Guadal area—the Guadal Formation is ~100 m thick in the Pampa Castillo section to the east and ~20 m thick in the Pampa Guadal section to the west, which suggests deposition in a half graben. These data are consistent with an extensional regime that resulted in progressive crustal thinning during deposition of the fluvial and volcanic deposits of the San José Formation and the subsequent transgression of marine waters of Atlantic origin during the time of maximum extension (Fig. 12D). Additional evidence in favor of an extensional regime during deposition of the Guadal Formation and correlative units is thoroughly discussed by Encinas et al. (2017) and is based on (1) the presence of late Oligocene–early Miocene volcano-sedimentary marine strata of the Ventana (41°S) and Traiguén (44°S–46°S) formations, which contain synextensional growth strata and geochemical signatures indicative of a thinned crust (Bechis et al., 2014; Litvak et al., 2014; Echaurren et al., 2016; Encinas et al., 2016a; Fernández Paz et al., 2017); (2) the occurrence of deep-marine strata (Fig. 4) of probable late Oligocene–early Miocene age west of the study area (Golfo de Penas, 47°S) with synextensional strata associated with normal faulting (Encinas et al., 2015); and (3) the presence of late Oligocene–early Miocene marine deposits in a large area that extends between the Pacific and the Atlantic coasts of Patagonia, including the western, central, and eastern parts of the present Patagonian Andes between ~41°S and 47°S (see Encinas et al., 2017 and references therein). This indicates that the elevated topography of the Patagonian Andes likely did not exist yet, precludes flexural subsidence as the principal driving mechanism for the marine transgression, and suggests a regional subsidence event driven by extensional tectonics. The presence of molluscan taxa of both putatively Pacific and Atlantic affinities in late Oligocene–early Miocene marine strata of the La Cascada Formation in the eastern flank of the North Patagonian Andes (43°S–44°S) supports this idea (Encinas et al., 2014). Maximum extension in Patagonia during the Oligocene–Miocene interval would enable such a transient connection between oceans and also challenges the existence of a mountain range. In this regard, Uliana and Biddle (1988) and Bechis et al. (2014) suggested a Pacific-Atlantic connection at the latitude of Meseta Guadal, where upper Oligocene–upper Miocene marine deposits of Pacific origin in the Golfo the Penas and Traiguén areas are closest to the coeval "Patagonian" deposits of Atlantic origin. However, this proposition is not yet supported by paleontologic studies as no mixed faunas of Atlantic and Pacific origin have been reported in any of these marine deposits on either side of the Andes.

After the "Patagonian" marine transgression, up to ~1000 m of early–middle Miocene (~19 Ma to 12 Ma) fluvial strata of the Santa Cruz Formation and younger units (e.g., Pedregoso and Río Mayo formations) were deposited in foreland basins developed in the eastern flank of the Andes and the extra-Andean region as a consequence of an important phase of compressive deformation and Andean uplift (Suárez and De La Cruz, 2000; Thomson, 2002; Lagabrielle et al., 2004; Blisniuk et al., 2005; Ramos and Ghiglione, 2008; Cuitiño et al., 2016) (Fig. 12E). The fluvial strata of the Santa Cruz Formation at the Meseta Guadal syncline are the only deposits in the entire Patagonian Andes that crop out within the Main Andean Cordillera. It is likely that correlative deposits occupied adjacent areas of this chain prior to uplift but were subsequently eroded. The fluvial units contain growth strata associated with folds and reverse faults that demonstrate their syntectonic origin (Lagabrielle et al., 2004; De La Cruz and Suárez, 2006). Paleocurrent analysis indicates a predominantly eastward direction, which requires that the source areas had to be located to the west of the sub-basins in question (Skarmeta, 1976; Ray, 1996; De La Cruz and Suárez, 2006; Rivas et al., 2015). The age of the Santa Cruz Formation in the western part of the extra-Andean region of Patagonia is ~1 Myr older than those of the same unit in the Atlantic coastal localities (see Cuitiño et al., 2016, and references therein) indicating the prograding character of these deposits triggered by the progressive uplift of the Andes during this time. Deposition of the Santa Cruz Formation and younger synorogenic strata finished at ~12 Ma (Guivel et al., 2006; De Iuliis et al., 2008; Rivas et al., 2015).

After the 19 Ma to 12 Ma contractional stage, a short period of rapid erosion and peneplanation followed that cross-cut the previous thrusts (Lagabrielle et al., 2007). Subsequently, extensive alkali flood basalts of the BSMCC and Meseta Lago Buenos Aires formations were extruded in a backarc setting to form large plateaus between 12.4 Ma and 7 Ma (Ramos and Kay, 1992; Gorring et al., 1997; Espinoza et al., 2005) (Fig. 12F). The basalts are not affected by reverse faults and overlie a flat surface that truncates early-middle Miocene thrusts (Lagabrielle et al., 2007). Late Miocene–Pliocene glacial and fluvioglacial deposits accumulated since ~7 Ma and are interbedded with younger basalts in the area (Lagabrielle et al., 2010). The alkaline-like geochemical signature of the flood basalts indicates an extensional setting (Espinoza et al., 2005) (Fig. 12F). Numerous authors have proposed that these basalts were associated with decompression melting of sub-slab asthenospheric mantle upwelling as result of a slab window (Ramos and Kay, 1992; Espinoza et al., 2005; references therein), like the BIMCC Formation. However, Guivel et al. (2006) argued that the subduction of the Chile Ridge at these latitudes (~48°S–46°S) started at ~6 Ma whereas the emplacement of the main plateau basalts took place between ~12.4 Ma and 5 Ma, which precludes a convincing cause-effect relationship. They proposed a model in which the collision of the southernmost segments of the Chile Ridge around 15 Ma caused a tear-in-the-slab that allowed the ascent of magmas derived from deep sub-slab asthenospheric mantle. During the last 5 Ma, the arrival of the Chile Ridge in the study area opened a true slab window that may have triggered the ascent of the most recent basaltic magmas (Guivel et al., 2006).

Although contractional deformation ceased at ~12 Ma in the Central Patagonian Andes, major uplift and topographic inversion occurred in this region after ~5 Ma (Lagabrielle et al., 2007). This event is not related to compressional tectonics but to an extensional/transtensional regime (Lagabrielle et al., 2007). Because this episode is coincident in time and space with the subduction of segments of the Chile Ridge at 6 Ma and 3 Ma, Lagabrielle et al. (2007) proposed that ridge subduction caused the ascent of the hot mantle, triggering doming and a weakening of the crust and causing localized collapse (Lagabrielle et al., 2007).

The total thickness of the Cenozoic succession in the study area includes ~2000 m of sedimentary and volcanic rocks that

accumulated over ~50 Myr. Of this, the synorogenic deposits of the Santa Cruz Formation and younger units, which were deposited in merely ~7 Ma, account for half of the total thickness (~1000 m). These data indicate that the tectonic setting during the rest of the Cenozoic, whether extensional or compressive, did not create significant accommodation space. This supports the idea that the 19–12 Ma interval was the only period characterized by significant Andean growth during the Cenozoic.

In their comprehensive study of the Central and North Patagonian Andes, Horton (2018b) (see also Horton et al., 2016; Horton, 2018a) noted that after a Late Cretaceous–Early Paleogene interval of pronounced Andean shortening, neutral to extensional conditions, spanning the forearc to retroarc, occurred between ~28°S and 43°S during the Paleogene as a consequence of mechanical decoupling. Neutral tectonic conditions in the western flank of the Andes at those latitudes gave way to diminished accumulation or to the development of a regional non-angular unconformity that was contemporaneous with extension in the magmatic arc and forearc provinces during the late Middle Eocene to earliest Miocene (Horton et al., 2016; Horton, 2018a,b). The "Rodados Lustrosos", a regional conglomerate < 2–20 m thick that crop out in the Central Andes at ~35°S, is a representative example of a highly condensed succession deposited during the ~40–20 Ma interval (Horton et al., 2016). Interestingly, a similar situation occurs in our study area. The Paleocene–early Miocene (~60–20 Ma) succession in the Central Patagonian Andes that includes the Ligorio Márquez, BIMCC, San José, and Guadal formations sums up to ~750 m. The succession deposited between ~40 Ma and 20 Ma which comprises at least part of the San José Formation and the Guadal Formation is only up to ~150 thick. In the extra-Andean region the coeval Sarmiento, San Julián, and Monte León formations sum up to ~600 m (Bellosi, 2010; Parras et al., 2012) whereas partially coeval units in the forearc probably sum up to more than ~1000 m (Forsythe and Nelson, 1985). Thus, similarly to the northern segments of the Andean Cordillera, the present hinterland of the Central Patagonian Andes was also characterized by reduced sedimentation rates, probably caused by mild extension, during the late Middle Eocene to earliest Miocene.

Our review indicates that clear evidence of compressive tectonics in the Central Patagonian Andes is limited to the Cretaceous–Paleocene? and to the early–middle Miocene (19–12 Ma) intervals, whereas extensional or neutral tectonic conditions appear to have dominated during most of the Cenozoic (Fig. 12). Some authors, however, have a different interpretation on the tectonic evolution of this area during this period. Ramos (1989) studied Cenozoic volcano-sedimentary rocks of the Posadas, Centinela, and Santa Cruz formations in the Central-Southern Patagonian Andes (47°S–49°S) at western Argentina and proposed that contractional deformation in this area took place between the Paleocene and the late Miocene based in his interpretation of the Cenozoic succession as molasse (synorogenic) deposits. However, subsequent studies based on geochemistry indicate that the Paleocene–Eocene flood basalts of the Posadas Formation (correlative with the BIMCC Formation) formed in an extensional setting (Espinoza et al., 2005). Ramos (1989) considered the "Patagonian" marine deposits of the Centinela Formation to be synorogenic, arguing that the inferred western seashore of the late Oligocene–early Miocene Atlantic transgression roughly matches the present foothills, indicating that uplift had begun in the Patagonian Cordillera at that time. However, the presence of uplifted strata of the Guadal Formation in the axial part of this range rules out this notion. Frassinetti and Covacevich (1999) assumed the existence of a mountain range that blocked the connection between the Pacific and Atlantic oceans in the Golfo de Penas and Meseta Guadal basins (~47°S) because of the invertebrate fossils of Atlantic origin that are present in the Guadal Formation. We argue that this only requires the presence of an emergent area between both basins, which could occur in any tectonic context and does not imply the presence of a compressional mountain range. Flint et al. (1994) proposed the occurrence of compressive deformation during deposition of the Guadal Formation, but do not indicate the presence of growth strata in this unit. Finally, based on thermochronologic data from southern Chile between 44°S and 51°S, Thomson et al. (2001) proposed accelerated cooling and denudation driven by compressive tectonics first in the forearc between 30 Ma and 23 Ma and then in the Patagonian Andes to the east between 12 Ma and 8 Ma. The Neogene group of cooling ages approximately matches deposition of synorogenic deposits of the Santa Cruz Formation and younger units but Thomson et al. (2001) proposed compressive tectonics in the forearc during the 30–23 Ma interval solely based in the lack of evidence for extensional tectonics. However, 26–23 Ma synextensional pillow basalts and turbidites of the Traiguén Formation and a 32 Ma volcanic breccia probably related to the same unit (Encinas et al., 2016a) crop out in the area sampled by Thomson et al. (2001). Therefore, an extensional regime better explains the Oligocene cooling ages.

7.4. Comparison of the Cenozoic tectonic evolution of the central, Northern, and Southern Patagonian Andes

The comparison of the tectonic evolution of the Central Patagonian Andes with the North Patagonian Andes reveals a largely parallel tectonic history. The North Patagonian Andes (39°S–43°30′S) only contain clear evidence for contractional deformation and Andean growth during the late Early Cretaceous to early Paleocene and the early-late Miocene (e.g., Orts et al., 2012; Echaurren et al., 2016). Bimodal volcanism included in the 60 Ma to 42 Ma Huitrera Formation (Rapela et al., 1988) has a within-plate signature (Aragón et al., 2013) and corresponds to synextensional strata associated with normal faults (Echaurren et al., 2016). This would indicate an extensional stage during the Paleocene–Eocene that has been attributed to the product of asthenospheric upwelling, presumably as a consequence of the subduction of the Aluk-Farallón spreading ridge (Aragón et al., 2013), or slab rollback (Echaurren et al., 2016). During the middle–late Eocene, 37 Ma arc activity resumes under extensional tectonics, as indicated by the 37 Ma growth strata of the Ventana Formation at the Rivadavia range (43°S) (Echaurren et al., 2016; Fernández Paz et al., 2018). Crustal thinning reached a maximum during the late Oligocene–early Miocene and resulted in the formation of several basins that extended from the present Chilean coast to the retroarc in Argentina between ~33°S–47°S, which filled with thick successions of volcanic and sedimentary rocks indicative of continental and marine settings (Muñoz et al., 2000; Jordan et al., 2001; Bechis et al., 2014; Litvak et al., 2014; Encinas et al., 2016a; Fernández Paz et al., 2017). Muñoz et al. (2000) attributed this episode to a major plate reorganization in the Southeast Pacific at ca. 28–26 Ma (Pardo-Casas and Molnar, 1987) that induced a transient period of vigorous asthenospheric wedge circulation and slab rollback of the subducting Nazca plate. Progressive extension and crustal thinning reached its maximum at ~20 Ma and led to marine flooding of much of Patagonia (Bechis et al., 2014; Encinas et al., 2016a, 2017). The marine transgression was followed by a phase of compressive tectonics beginning at ~19–16 Ma that resulted in the emergence, uplift, and deformation of the late Oligocene–early Miocene marine strata, the deposition of synorogenic continental and marine sediments, and the growth of the Patagonian Andes (Orts et al., 2012; Bilmes et al., 2013; Bechis et al., 2014; Echaurren et al., 2016; Encinas et al., 2017).

In contrast with the evolution of the North and Central Patagonian Andes, the Southern Patagonian (or Austral) Andes are generally thought to have been the subject of compressive deformation and foreland sedimentation from the late Early Cretaceous to present time interval (e.g., Biddle et al., 1986). However, some authors postulate intervals of extensional tectonics during parts of the Cenozoic, at least for the southernmost part of this chain (e.g., Ghiglione, 2016b). The evolution of the northern (~47°S–52°S) and the southern (~52°S–56°S) parts of the Southern Patagonian Andes show some differences, probably due to the influence of the opening of the Scotia Sea on the southern tip of South America.

Orogenic growth and related foreland sedimentation in the northern part of the Southern Patagonian Andes (47°S–52°S) began around 101–88 Ma (Varela et al., 2012). Compressive deformation during the Paleogene is proposed by Malumián et al. (2000) based on the presence of progressive unconformities on the 47–26 Ma Río Turbio Formation and the 23.5 Ma Río Guillermo Formation (radiometric ages from Fosdick et al., 2015). These syntectonic sequences onlap the ~60 Ma Cerro Dorotea Formation (Ghiglione et al., 2016a), bracketing an upper Paleocene–lower Eocene hiatus spanning from 60 to 47 Ma (Malumián et al., 2000). The late Oligocene–early Miocene "Patagonian" Atlantic marine transgression has been interpreted as deposited in a foreland basin whereas fast infilling of the accommodation space resulted in progradation of synorogenic fluvial deposits of the early–middle Miocene Santa Cruz Formation (Blisniuk et al., 2005; Cuitiño et al., 2016).

The Cenozoic tectonic development of the southern part of the Southern Patagonian Andes (52°S–56°S, also known as the Fueguian Andes) occurred amidst a composite kinematic regime. Andean uplift and compression were sustained due to continuous subduction, whereas strike-slip and extensional tectonics occurred during the opening of the Scotia Sea and the northward drift of South America during its separation with the Antarctic Peninsula (Lagabrielle et al., 2009; Ghiglione, 2016b, and references therein). Structural and geophysical data from the Fueguian fold and thrust belt indicate Paleocene–Early Eocene continental stretching (Ghiglione et al., 2008) that can be connected to the development of Paleocene extensional depocenters in the Austral and offshore basins associated with the slow separation of the South American and Antarctica plates (Ghiglione, 2016b, and references therein). It was followed by a period of basement uplift and propagation of the fold and thrust belt during the middle to late Eocene, as indicated by the analysis of growth strata, fission track data, and U-Pb detrital zircon geochronology (Ghiglione and Ramos, 2005; Barbeau et al., 2009; Gombosi et al., 2009). Syntectonic sequences have also been recognized in Oligocene strata (e.g., Ghiglione et al., 2010). Subsequently, relative movement between South America and Antarctica was accommodated by spreading in the West Scotia Sea from about 28 Ma until ~16 Ma when the Scotia Plate started to move independently of the South American plate (Lagabrielle et al., 2009) along a sinistral strike-slip fault zone (Ghiglione, 2016b and references therein). Strike-slip deformation has persisted in the southernmost Andes since the Oligocene (Ghiglione, 2016b).

This review of the regional geologic literature indicates that the tectonic evolution of the Central and Northern Patagonian Andes are basically similar while the history of the Southern Patagonian Andes is fundamentally different. It appears that the northern and central segments were subjected to alternating phases of compressional and extensional deformation during the Cenozoic whereas the southern segment was mostly dominated by compressive tectonics, Andean growth, and foreland deposition during that period. It is possible that there is a change in the tectonic behavior of the segments located north and south of ~47°S during the Cenozoic. However, such a change is difficult to explain considering that convergence conditions have been rather similar in both segments during most of the Cenozoic (e.g., Pardo-Casas and Molnar, 1987). Another possibility is that some of the mentioned tectonic interpretations (including ours) are erroneous and that the Central and Northern Patagonian Andes were dominated by compressive deformation during the entire Cenozoic or that the Southern Patagonian Andes were subjected to alternating phases of compressional and extensional deformation during that period. Our data are not conclusive and do not allow us to solve this problematic for the moment. However, the geochemistry of the volcanic rocks from the BIMCC and San José formations and the presence of marine deposits of the Guadal Formation in the eastern and axial parts of the Central Patagonian Andes are important evidence in favor of thin crust and against topographic growth of the Andes, at least during most of the early Eocene–early Miocene interval. It appears that compressional tectonics in this Andean segment during the Cenozoic was almost limited to a short interval between ~19 Ma and 12 Ma. Rodríguez Tribaldos et al. (2017) reached a similar conclusion using quantitative drainage analysis. They proposed that uplift in the Central Patagonian Andes was minor until ~20 Ma, coinciding with the transit between marine deposition of the Guadal Formation and synorogenic fluvial sedimentation of the Santa Cruz Formation. The occurrence of the late Oligocene–early Miocene marine deposits of the Guadal Formation strata at ~1700 m a.m.s.l. (see De la Cruz and Suárez, 2008) in the Chile Chico area provides additional evidence for recent uplift. Interestingly, data based on fossil mammals, paleobotanical, and palynological studies (Ortiz-Jaureguizar and Cladera, 2006; Barreda and Palazzesi, 2007; Palazzesi and Barreda, 2012) indicate that the Patagonian Andes, including the southern segment of this range, did not attained the sufficient height as to cause an important orographic rain shadow effect that considerably increased the aridity in the eastern foreland until the middle-late Miocene. In addition, recent studies based on K-Ar dating on synkinematically formed illite in low-grade metamorphic pelites from the Southern Patagonian Andes (51°S–52°S) indicate low exhumation rates for this area between 46.5 Ma and 22 Ma suggesting a period of geological quiescence (Süssenberger et al., 2017). These data suggests that Cenozoic Andean growth in the entire Patagonian Andes was not significant until the early Miocene. We anticipate future studies that will improve our understanding of the differences in the tectonic evolution of the northern, central, and southern segments of the Patagonian Andes during the Cenozoic.

8. Conclusions

In order to better understand the geologic evolution of the Central Patagonian Andes during the Cenozoic, we carried out geochronologic, provenance, stratigraphic, sedimentologic, and geochemical studies on the sedimentary and volcanic deposits that crop out at the Meseta Guadal and Chile Chico areas (~47°S).

Our geochronologic data indicate the presence of a nearly complete Cenozoic record in the Central Patagonian Andes, which refutes previous interpretations of a hiatus between the middle Eocene and late Oligocene. The successions of the two studied areas present stratigraphic differences. The Chile Chico succession is exposed in the eastern flank of the Andes and crops out in a plateau limited to the east by the Jeinemeni reverse fault. West of this fault, a concordant succession of Cenozoic sedimentary and volcanic strata includes fluvial deposits of the upper Paleocene–lower Eocene Ligorio Márquez Formation, basaltic rocks of the Eocene Basaltos Inferiores de la Meseta Chile Chico Formation, marine strata of the upper Oligocene–lower Miocene Guadal Formation, and middle Miocene–Pliocene basaltic rocks of the Basaltos

Superiores de la Meseta de Chile Chico and Pico Sur formations. East of the Jeinemeni fault the succession comprises the same units but the lower–middle Miocene Santa Cruz Formation overlies the Guadal Formation and underlies the basalts of the Meseta Lago Buenos Aires Formation, which is correlative with the BSMCC Formation.

The Meseta Guadal succession constitutes the only record of Cenozoic deposits in the axial part of the Patagonian Andes. The Cenozoic rocks form a concordant succession including middle Eocene–upper Oligocene fluvial strata of the San José Formation, upper Oligocene–lower Miocene marine deposits of the Guadal Formation, and lower–middle Miocene fluvial strata of the Santa Cruz Formation.

We carried out the first geochemical analysis on volcanic rocks of the San José Formation. Our results indicate that this volcanism is linked to an arc-like setting with tholeiitic to calc-alkaline sources and clear slab-derived fluid input. Trace element ratios suggest their equilibrium at pressures consistent with crust of normal to attenuated thickness, similar to late Oligocene–early Miocene arc-derived volcanism developed within the extensional setting of the Traiguen and Ventana formations. This arc-like volcanism contrasts with Eocene to Oligocene alkaline magmatism registered in the Andean and extra-Andean regions at the same latitude. The latter is mostly associated with a typical intraplate setting, characterized by deeper E-MORB sources.

The Ligorio Márquez Formation shows a subtle angular unconformity with Upper Jurassic–Lower Cretaceous strata of the El Toqui Formation, which reflects compressive deformation during part of the Cretaceous–Paleocene interval. Cenozoic units that crop out in the study area present conformable or paraconformable contact relationships among them, which suggests the absence of significant compressive deformation during this period. We only identified growth strata in the synorogenic fluvial deposits of the early-middle Miocene Santa Cruz Formation and younger units in the area. Although our data are not conclusive, geochemical studies and stratigraphic considerations suggest that the fluvial strata and the flood basalts of the Ligorio Márquez and the BIMCC formations were probably formed during an extensional phase related to the subduction of the Aluk-Farallon spreading ridge during the late Paleocene to Eocene. Geochemical data suggest that the San José Formation was deposited in an extensional setting during the middle Eocene to late Oligocene. Progressive crustal thinning probably allowed the transgression of marine waters of Atlantic origin and deposition of the Guadal Formation sediments during the late Oligocene–early Miocene. The fluvial synorogenic strata of the Santa Cruz Formation and younger units were deposited during compressive deformation and Andean uplift during the early-middle Miocene. Finally, published geochemical data suggest that the alkali flood basalts of the middle Miocene–Pliocene Basaltos Superiores de la Meseta Chile Chico and Meseta Lago Buenos Aires formations and younger units were extruded in the area in response to the suduction of the Chile Ridge under an extensional regime.

Our studies show that clear evidence of compressive tectonics in the Central Patagonian Andes is limited to the Late Cretaceous–Paleocene (?) and the early–middle Miocene (~19–12 Ma) intervals, whereas extensional or neutral tectonic conditions appear to have dominated most of the Cenozoic. This tectonic evolution is similar to that ascribed to the North Patagonian Andes. In contrast, the Southern Patagonian Andes is generally thought to have been the subject of compressive deformation and foreland sedimentation from the late Early Cretaceous to present time interval. These data suggest a change in the tectonic behavior of the Patagonian Andes north and south of ~47°S. Despite this, some studies suggest that the evolution of the Southern Patagonian Andes does not differ substantially from that of the Northern and Central segments. Further studies should be carried out in order to accurately understand the differences in the Cenozoic tectonic evolution of the northern, central, and southern parts of the Patagonian Andes.

Acknowledgments

This research was funded by Fondecyt Projects (Nos. 1151146 and 1110914), Programa de Fomento y Transferencia tecnológica en Exploración Minera, código BIP No 30114940-0, PIP CONICET 2015–2017 No. 11220150100426, UBACYT 2015–2017 No. 20020150100166BA, PICT 2016 No. 2252, NSF EAR-165031, and the Yale Institute for Biospheric Studies. We thank the help of Parque Patagonia and especially of Cristian Saucedo, Marcos Asensio, Eduardo Castro, and the late Douglas Tompkins. We acknowledge the help of Gabriel Carrasco during fieldwork. We thank to Luis Buatois and Luciano Zapata for their help in the identification of some of the trace fossils from the Guadal and Santa Cruz formations and to Aníbal Anavalón, who helped in the drawing of some figures. We are grateful to Damian Nance, Brian Horton, Yves Lagabrielle, and an anonymous reviewer for their helpful suggestions and constructive comments, which considerably improved the manuscript.

Appendix A. Supplementary data

Supplementary data related to this article can be found at https://doi.org/10.1016/j.gsf.2018.07.004.

References

Anma, R., Armstrong, R., Danhara, T., Orihashi, Y., Iwano, H., 2006. Zircon sensitive high mass-resolution ion microprobe U-Pb and fission-track ages for gabbros and sheeted dykes of the Taitao Ophiolite, Southern Chile, and their tectonic implications. The Island Arc 15, 130–142.

Aragón, E., Pinotti, L., D'eramo, F., Castro, A., Rabbia, O., Coniglio, J., Demartis, M., Hernando, I., Cavarozzi, C.E., Aguilera, Y.E., 2013. The Farallon-Aluk ridge collision with South America: implications for the geochemical changes of slab window magmas from fore- to back-arc. Geoscience Frontiers 4, 377–388.

Baker, P.E., Rea, W.J., Skarmeta, J., Caminos, R., Rex, D.C., 1981. Igneous history of the andean Cordillera and patagonian plateau around latitude 46°S. Philosophical Transactions of the Royal Society of London. Series A, Mathematical and Physical Sciences A303, 105–149.

Barbeau, D.L., Olivero, E., Swanson-Hysell, N., Zahid, K., Murray, K., Gehrels, G., 2009. Detrital-zircon geochronology of the eastern magallanes foreland basin: implications for eocene kinematics of the northern Scotia arc and drake passage. Earth and Planetary Science Letters 20, 23–45.

Barreda, V., Palazzesi, L., 2007. Patagonian vegetation turnovers during the Paleogene-early Neogene: origin of arid-adapted floras. The Botanic Review 73, 31–50.

Bechis, F., Encinas, A., Concheyro, A., Litvak, V.D., Aguirre-Urreta, B., Ramos, V.A., 2014. New age constraints for the Cenozoic marine transgressions of northwestern Patagonia, Argentina (41°–43°S): paleogeographic and tectonic implications. Journal of South American Earth Sciences 52, 72–93.

Bellosi, E.S., 2010. Physical stratigraphy of the Sarmiento Formation (middle eocene – lower Miocene) at gran Barranca, central Patagonia. In: Madden, R.H., Carlini, A.A., Vucetich, M.G., Kay, R.F. (Eds.), The Paleontology of Gran Barranca: Evolution and Environmental Change through the Middle Cenozoic of Patagonia. Cambridge University Press, Cambridge, UK, pp. 19–31.

Biddle, K.T., Uliana, M.A., Mitchum, R.M., Fitzgerald, M.G., Wright, R.C., 1986. The stratigraphy and structural evolution of the central and eastern Magallanes Basin, southern South America. In: Allen, A., Homewood, P. (Eds.), Foreland Basins, 8. Blackwell Scientific Publications, London. International Association of Sedimentologists, Special Publication, pp. 41–61.

Bilmes, A., D'Elia, L., Franzese, J., Veiga, G., Hernández, M., 2013. Miocene block uplift and basin formation in the Patagonian foreland: the Gastre Basin, Argentina. Tectonophysics 601, 98–111.

Blisniuk, P.M., Stern, L.A., Chamberlain, C.P., Idelman, B., Zeitler, K., 2005. Climatic and ecologic changes during Miocene surface uplift in the southern patagonian Andes. Earth and Planetary Science Letters 230, 125–142.

Bostelmann, E., Buldrini, K., 2012. Late-early Miocene fossil mammals of the Pampa Guadal area, Meseta Cosmelli, Aysén region, Chilean Patagonia. In: Leppe, M., Aravena, J.C., Villa-Martínez, R. (Eds.), Abriendo ventanas al pasado, III Simposio de Paleontología en Chile, 3. resúmenes, Punta Arenas, pp. 38–41.

Bourgois, J., Martin, H., Lagabrielle, Y., Le Moigne, J., Jara, J.F., 1996. Subduction erosion related to spreading-ridge subduction: Taitao peninsula (Chile margin triple junction area). Geology 24, 723–726.
Breen, P., Lichtin, S., Super, J., Auerbach, D.J., Brandon, M., 2015. Reconstructing paleocene-eocene patagonian paleoclimate: organic proxy data from the Ligorio Márquez Formation. GSA Abstracts with Programs 47, 562.
Breitsprecher, K., Thorkelson, D.J., 2009. Neogene kinematic history of Nazca-Antarctic-phoenix slab windows beneath Patagonia and the Antarctic peninsula. Tectonophysics 464, 10–20.
Bruni, S., D'Orazio, M., Haller, M.J., Innocenti, F., Manetti, P., Pécskay, Z., Tonarini, S., 2008. Time-evolution of magma sources in a continental back-arc setting: the Cenozoic basalts from Sierra de San Bernardo (Patagonia, Chubut, Argentina). Geological Magazine 145, 714–732.
Cande, S.C., Leslie, R.B., 1986. Late Cenozoic tectonics of the southern Chile trench. Journal of Geophysical Research 91, 471–496.
Chang, Z., Vervoort, J.D., McClelland, W.C., Knaack, C., 2006. U-Pb dating of zircon by LA-ICP-MS. Geochemistry, Geophysics, Geosystems 7, 1–14.
Charrier, R., Linares, E., Niemeyer, H., Skarmeta, J., 1979. K-Ar ages of basalt flows of the Meseta Buenos Aires in southern Chile and their relation to the southeast Pacific triple junction. Geology 7 (9), 436–439.
Charrier, R., Baeza, O., Elgueta, S., Flynn, J.J., Gans, P., Kay, S.M., Muñoz, N., Wyss, A.R., Zurita, E., 2002. Evidence for Cenozoic extensional basin development and tectonic inversion south of the flat-slab segment, southern Central Andes, Chile (33°–36°S.L.). Journal of South American Earth Sciences 15, 117–139.
Clyde, W., Wilf, P., Iglesias, A., Slingerland, R.L., Barnum, T., Bijl, P.K., Bralower, T.J., Brinkhuis, H., Comer, E.M., Huber, B.T., Ibañez-Mejia, M., Jicha, B.R., Krause, J.M., Schueth, J.D., Singer, B.S., Raigemborn, M.S., Schmitz, M.D., Sluijs, A., Zamaloa, M.C., 2014. New age constraints for the salamanca formation and lower Río Chico group in the western san Jorge basin, Patagonia, Argentina: implications for cretaceous-paleogene extinction recovery and land mammal age correlations. The Geological Society of America Bulletin 126 (3–4), 289–306.
Cuitiño, J.I., Ventura Santos, R., Alonso Muruaga, P.J., 2015. Sr-stratigraphy and sedimentary evolution of early Miocene marine foreland deposits in the northern Austral (Magallanes) Basin, Argentina. Andean Geology 42 (3), 64–385.
Cuitiño, J.I., Fernicola, J.C., Kohn, M.J., Trayler, R., Naipauer, M., Bargo, M.S., Kay, R., Vizcaíno, S.F., 2016. U-Pb geochronology of the Santa Cruz formation (early Miocene) at the Río Bote and Río Santa Cruz (southernmost Patagonia, Argentina): implications for the correlation of fossil vertebrate localities. Journal of South American Earth Sciences 70, 198–210.
De Iuliis, G., Brandoni, D., Scillato-Yané, G.J., 2008. New remains of Megathericulus patagonicus Ameghino, 1904 (Xenarthra, Megatheriidae): information on primitive features of megatheriines. Journal of Vertebrate Paleontology 28, 181–196.
De la Cruz, R., Suárez, M., Morata, D., Espinoza, F., Troncoso, A., 2003. El Cenozoico del Lago General Carrera, Aysén, Chile (46°30'-47°15'S): estratigrafía y tectónica. X Congreso Geológico Chileno, Concepción, p. 9 (in Spanish).
De la Cruz, R., Welkner, D., Suárez, M., Quiroz, D., 2004. Geología del área Oriental de la Hojas Cochrane y Villa O'Higgins, Región Aisén del General Carlos Ibáñez del Campo. Carta Geológica de Chile Serie Geología Básica, vol. 85. Servicio Nacional de Geología y Minería, Santiago, Chile, p. 57 scale 1:250000 (in Spanish).
De La Cruz, R., Suárez, M., 2006. Geología del área Puerto Guadal-Puerto Sánchez, Región Aisén del General Carlos Ibañez del Campo. Carta Geológica de Chile, Serie Geología Básica, vol. 95. Servicio Nacional de Geología y Minería, Santiago, Chile, p. 58 scale 1:100000 (in Spanish).
De la Cruz, R., Suárez, M., 2008. Geología del Área de Chile Chico-Río de Las Nieves, Región de Aisén del General Carlos Ibáñez del Campo. Carta Geológica de Chile, Serie Geología Básica, vol. 112. Servicio Nacional de Geología y Minería, Santiago, Chile, p. 67. Scale 1:100000. (in Spanish).
De la Cruz, R., Cortés, J.C., 2011. Geología del área oriental de la Hoja Puerto Cisnes. Región de Aisén del General Carlos Ibáñez del Campo. Carta Geológica de Chile, Serie Geología Básica, vol. 127. Servicio Nacional de Geología y Minería, Santiago, Chile, p. 70. Scale 1:100.000. (in Spanish).
Echaurren, A., Folguera, A., Gianni, G., Orts, D., Tassara, A., Encinas, A., Gimenez, M., Valencia, V., 2016. Tectonic evolution of the North Patagonian Andes (41°-44°S) through recognition of syntectonic strata. Tectonophysics 677–678, 99–114.
Ecosteguy, L., Dal Molín, C., Franchi, M., Geuna, S., Lapido, O., 2003. Hoja Geológica 4772-II, Lago Buenos Aires, Provincia de Santa Cruz. Boletín del Servicio Geológico Argentino 339. Programa Nacional de Cartas Geológicas de la República Argentina scale 1:250.000. (in Spanish).
Encinas, A., Zambrano, P.A., Finger, K.L., Valencia, V., Buatois, L.A., Duhart, P., 2013. Implications of deep-marine Miocene deposits on the evolution of the north patagonian Andes. Journal of Geology 121, 215–238.
Encinas, A., Pérez, F., Nielsen, S.N., Finger, K.L., Valencia, V., Duhart, P., 2014. Geochronologic and paleontologic evidence for a pacific–Atlantic connection during the late oligocene–early Miocene in the patagonian Andes (43°–44°S). Journal of South American Earth Sciences 55, 1–18.
Encinas, A., Moreira, R., Nielsen, S., Bravo, X., 2015. Estratigrafía, edad y ambiente de sedimentación de los depósitos Neógenos del Golfo de Penas y Península de Taitao sur de Chile (47°S). XIV Congreso geológico Chileno Coquimbo Actas 1–4, 269 (in Spanish).
Encinas, A., Folguera, A., Oliveros, V., De Girolamo Del Mauro, L., Tapia, F., Riffo, R., Hervé, F., Finger, K.L., Valencia, V.A., Gianni, G., Álvarez, O., 2016a. Late Oligocene–early Miocene submarine volcanism and deep-marine sedimentation in an extensional basin of southern Chile: implications for the tectonic development of the North Patagonian Andes. The Geology Society of America Bulletin 128, 807–823. https://doi.org/10.1130/B31303.1.
Encinas, A., Folguera, A., Litvak, V.D., Echaurren, A., Gianni, G., Fernández Paz, L., Bobe, R., Valencia, V.A., 2016b. New age constraints for the cenozoic deposits of the Patagonian Andes and the Sierra de San Bernardo between 43° and 46°S. In: Primer Simposio de Tectónica Sudamericana, Santiago.
Encinas, A., Folguera, A., Bechis, F., Finger, K.L., Zambrano, P., Pérez, F., Bernabé, P., Tapia, F., Riffo, R., Buatois, L., Orts, D., Nielsen, S.N., Valencia, V.A., Cuitiño, J., Oliveros, V., De Girolamo Del Mauro, L., Ramos, V.A., 2017. The late Oligocene-early Miocene marine transgression of Patagonia. In: Folguera, A., Contreras Reyes, E., Heredia, N., Encinas, A., Iannelli, S., Oliveros, V., Dávila, F., Collo, G., Giambiagi, L., Maksymowicz, A., Iglesia Llanos, P., Turienzo, M., Naipauer, M., Orts, D.,M., Litvak, V., Alvarez, O., Arriagada, C. (Eds.), The Making of the Chilean-argentinean Andes.
Espinoza, F., Morata, D., 2003. Petrogenesis de los basaltos Cenozoicos de la Meseta Chile Chico, XI Región de Aysén, Chile. X Congreso Geológico Chileno, Concepción (in Spanish).
Espinoza, F., Morata, D., Pelleter, E., Maury, R.C., Suárez, M., Lagabrielle, Y., Polvé, M., Bellon, H., Cotten, J., De la Cruz, R., Guivel, C., 2005. Petrogenesis of the Eocene and Mio-Pliocene alkaline basaltic magmatism in Meseta Chile Chico, southern Patagonia, Chile: evidence for the participation of two slab windows. Lithos 82, 315–343.
Fernández Paz, L., Bechis, F., Litvak, V.D., Echaurren, A., Iannelli, S., Encinas, A., Oliveros, V., Folguera, A., Valencia, V., 2017. Evolución del volcanismo de arco durante el Eoceno medio-Mioceno temprano en los Andes Patagónicos. 20°. Congreso Geológico Argentino, p. 6 (in Spanish).
Fernández Paz, L., Litvak, V.D., Echaurren, A., Iannelli, S.B., Encinas, A., Folguera, A., Valencia, V., 2018. Late eocene volcanism in North Patagonia (42°30'–43°S): arc resumption after a stage of within-plate magmatism. Journal of Geodynamics 113, 13–31.
Flint, S.S., Prior, D.J., Agar, S.M., Turner, P., 1994. Stratigraphic and structural evolution of the Tertiary Cosmelli Basin and its relationship to the Chile triple junction. Journal of the Geological Society 151, 251–268.
Flynn, J.J., Novacek, M.J., Dodson, H.E., Frassinetti, D., McKenna, M.C., Norell, M.A., Sears, K.E., Swisher, C.C., Wyss, A.R., 2002. A new fossil mammal assemblage from the southern Chilean Andes: implications for geology, geochronology, and tectonics. Journal of South American Earth Sciences 15, 285–302.
Forsythe, R., Nelson, E., 1985. Geological manifestations of ridge collision: evidence from the Golfo de Penas-Taitao Basin, southern Chile. Tectonics 4, 477–495.
Fosdick, J.C., Bostelmann, J.E., Leonard, J., Ugalde, R., Oyarzún, J.L., Griffin, M., 2015. Timing and Rates of Foreland Sedimentation: New Detrital Zircon U/Pb Geochronology of the Cerro Dorotea, Río Turbio, and Río Guillermo Formations, Magallanes Basin. XIV Congreso Geológico Chileno, La Serena.
Frassinetti, D., Covacevich, V., 1999. Invertebrados fósiles marinos de la Formación Guadal (Oligoceno Superior-Mioceno Inferior) en Pampa Castillo, Región de Aisén, Chile, vol. 51. Subdirección Nacional de Geología, Sernageomín, p. 96 (in Spanish).
Gaschnig, R.M., Vervoort, J.D., Lewis, R.S., McClelland, W.C., 2010. Migrating magmatism in the northern US Cordillera: in situ U–Pb geochronology of the Idaho batholith. Contributions to Mineralogy and Petrology 159 (6), 863–883.
Gehrels, G., Valencia, V., Pullen, A., 2006. Detrital zircon geochronology by laser ablation multicollector ICPMS at the Arizona LaserChron center. Emerging opportunities. The Paleontological Society Papers 12, 67–76.
Ghiglione, M.C., Ramos, V.A., 2005. Chronology of deformation in the Southernmost Andes of Tierra del Fuego. Tectonophysics 405, 25–46.
Ghiglione, M.C., Yagupsky, D., Ghidella, M., Ramos, V.A., 2008. Continental stretching preceding the opening of the drake passage: evidence from Tierra del Fuego. Geology 36, 643–646.
Ghiglione, M.C., Quinteros, J., Yagupsky, D., Bonillo-Martínez, P., Hlebszevtich, J., Ramos, V.A., Vergani, G., Figueroa, D., Quesada, S., Zapata, T., 2010. Structure and tectonic history of the foreland basins of southernmost South America. Journal of South American Earth Sciences 29, 262–277.
Ghiglione, M.C., Ramos, V.A., Cuitiño, J., Barberón, V., 2016a. Growth of the Southern Patagonian Andes (46°–53°S) and their relation to subduction processes. In: Folguera, A., Naipauer, M., Sagripanti, L., Ghiglione, M.C., Orts, D.L., Giambiagi, L. (Eds.), Growth of the Southern Andes. Springer Earth System Sciences, pp. 201–240.
Ghiglione, M.C., 2016b. Orogenic growth of the Fuegian Andes (52°–56°) and their relation to tectonics of the Scotia arc. In: Folguera, A., Naipauer, M., Sagripanti, L., Ghiglione, M.C., Orts, D.L., Giambiagi, L. (Eds.), Growth of the Southern Andes. Springer Earth System Sciences, pp. 241–268.
Gianni, G., Navarrete, C., Orts, D., Tobal, J., Folguera, A., Giménez, M., 2015. Patagonian broken foreland and related synorogenic rifting: the origin of the Chubut Group Basin. Tectonophysics 649, 81–99.
Gianni, G.M., Echaurren, A., Folguera, A., Likerman, J., Encinas, A., Dal Molin, C., Valencia, V.A., 2017a. Tectónica de intraplaca en Patagonia: Registro de la deformación Andina en una placa continental débil. LATINTEC (in Spanish).
Gianni, G.M., Echaurren, A., Folguera, A., Likerman, J., Encinas, A., García, H.P.A., Dal Molin, C., Valencia, V.A., 2017b. Cenozoic intraplate tectonics in Central Patagonia: record of main Andean phases in a weak upper plate. Tectonophysics 721, 151–166.
Gill, J.B., 1981. Orogenic Andesites and Plate Tectonics, Minerals and Rocks. Springer-Verlag, Berlin, Heidelberg, New York, p. 390.

Gombosi, D.J., Barbeau, D.L., Garver, J., 2009. New thermochronometric constraints on the rapid Paleogene exhumation of the Cordillera Darwin complex and related thrust sheets in the Fuegian Andes. Terra Nova 21, 507–515.
Gorring, M., Kay, S., Zeitler, P., Ramos, V., Rubiolo, D., Fernández, M., Panza, J., 1997. Neogene patagonian Plateau Lavas: continental magmas associated with ridge collision at the Chile triple junction. Tectonics 16 (1), 1–17.
Guivel, C., Morata, D., Pelleter, E., Espinoza, F., Maury, R.C., Lagabrielle, Y., Polvé, M., Bellon, H., Coiten, J., Benoit, M., Suárez, M., De la Cruz, R., 2006. Miocene to Recent Patagonian basalts (46°-47°S): geochronometric and geochemical evidence for slab tearing during ridge collision. Journal of Volcanology and Geothermal Research 149 (3–4), 346–370.
Heim, A., 1940. Geological observations in the patagonian Cordillera (preliminary report). Eclogae Geologicae Helvetiae 33, 25–51.
Hervé, F., 1994. The southern Andes between 39° and 44°S latitude: the geological signature of a transpressive tectonic regime related to a magmatic arc. In: Reutter, K.J., Scheuber, E., Wigger, P. (Eds.), Tectonics of the southern Central Andes. Springer-Verlag, Berlin, pp. 243–248.
Hervé, F., Pankhurst, R.J., Drake, R., Beck, M.E., 1995. Pillow metabasalts in a mid-Tertiary extensional basin adjacent to the Liquiñe-Ofqui fault zone: the Isla Magdalena area, Aysén, Chile. Journal of South American Earth Sciences 8 (1), 33–46.
Hervé, F., Fanning, C.M., Pankhurst, R.J., 2003. Detrital zircon age patterns and provenance of the metamorphic complexes of southern Chile. Journal of South American Earth Sciences 16 (1), 33–46.
Hildreth, W., Moorbath, S., 1988. Crustal contributions to arc magmatism in the Andes of Central Chile. Contributions to Mineralogy and Petrology 98, 455–489.
Horton, B.K., 2018a. Sedimentary record of Andean mountain building. Earth Science Reviews 178, 279–309.
Horton, B.K., 2018b. Tectonic regimes of the central and southern Andes: responses to variations in plate coupling during subduction. Tectonics 37, 402–429.
Horton, B.K., Fuentes, F., Boll, A., Starck, D., Ramirez, S.G., Stockli, D.F., 2016. Andean stratigraphic record of the transition from backarc extension to orogenic shortening: a case study from the northern Neuquén Basin, Argentina. Journal of South American Earth Sciences 71, 17–40.
Introcaso, A., Pacino, M.C., Guspi, F., 2000. The Andes of Argentina and Chile: crustal configuration, isostasy, shortening and tectonic features from gravity data. Temas de Geociencias 5, 31.
Jordan, T., Matthew, W., Veiga, R., Pángaro, F., Copeland, P., Kelley, S., Mpodozis, C., 2001. Extension and basin formation in the southern Andes caused by increased convergence rate: a mid-Cenozoic trigger for the Andes. Tectonics 20, 308–324.
Kay, S.M., Ramos, V.A., Gorring, M.L., 2002. Geochemistry of Eocene plateau basalts related to ridge collision in southern Patagonia. In: XV Congreso Geológico Argentino, El Calafate, pp. 60–65.
Kay, S.M., Ardolino, A.A., Gorring, M.L., Ramos, V.A., 2007. The somuncura large igneous province in Patagonia: interaction of a transient mantle thermal anomaly with a subducting slab. Journal of Petrology 48, 43–77. https://doi.org/10.1093/petrology/egl053.
Krause, J.M., Clyde, W.C., Ibáñez-Mejía, M., Schmitz, M.D., Barnum, T., Bellosi, E.S., Wilf, P., 2017. New age constraints for early Paleogene strata of central Patagonia, Argentina: implications for the timing of south American land mammal ages. Geological Society of America Bulletin 129 (7–8), 886–903.
Kuiper, K., Deino, A., Hilgen, F., Krijgsman, W., Renne, P., Wijbrans, J., 2008. Synchronizing rock clocks of Earth history. Science 320, 500–504.
Lagabrielle, Y., Suárez, M., Rossello, E.A., Hérail, G., Martinod, J., Régnier, M., De la Cruz, R., 2004. Neogene to quaternary tectonic evolution of the patagonian Andes at the latitude of the Chile triple junction. Tectonophysics 385, 211–241.
Lagabrielle, Y., Suarez, M., Malavieille, J., Morata, D., Espinoza, F., Maury, R.C., Scalabrino, R., Barbero, L., de la Cruz, R., Rossello, E., Bellon, H., 2007. Pliocene extensional tectonics in the Eastern Central Patagonian Cordillera: geochronological constraints and new field evidence. Terra Nova 19, 413–424.
Lagabrielle, Y., Goddéris, Y., Donnadieu, Y., Malavieille, J., Suarez, M., 2009. The tectonic history of Drake Passage and its possible impacts on global climate. Earth and Planetary Science Letters 279, 197–211.
Lagabrielle, Y., Scalabrino, B., Suarez, M., Ritz, J.F., 2010. Mio-Pliocene glaciations of Central Patagonia: new evidence and tectonic implications. Andean Geology 37, 276–299.
Lamb, S., Davis, P., 2003. Cenozoic climate change as a possible cause for the rise of the Andes. Nature 425, 792–797.
Lee, J.Y., Marti, K., Severinghaus, J.P., Kawamura, K., Yoo, H.S., Lee, J.B., Kim, J.S., 2006. A redetermination of the isotopic abundances of atmospheric Ar. Geochimica et Cosmochimica Acta 70, 4507–4512.
Litvak, V.D., Encinas, A., Oliveros, V., Bechis, F., Folguera, A., y Ramos, V.A., 2014. El volcanismo mioceno inferior vinculado con las ingresiones marinas en los Andes Nordpatagónicos. XIX Congreso Geológico Argentino, Córdoba, Actas CD, p. 2 (in Spanish).
Ludwig, K.R., 2003. Users Manual for Isoplot 3.00: a Geochronological Toolkit for Microsoft Excel. Berkeley Geochronology Center, vol. 4. Especial Publicaction, p. 71.
Malumián, N., Panza, J.L., Parisi, C., Nañez, C., Caramés, A., Torre, E., 2000. Hoja Geológica 5172-III-Yacimiento Río Turbio, provincia Santa Cruz, 1:250.000, vol. 247. Servicio Geológico Minero Argentino, Boletín, p. 108 (in Spanish).
Martinod, J., Husson, L., Roperch, P., Guillaume, B., Espurt, N., 2010. Horizontal subduction zones, convergence velocity and the building of the Andes. Earth and Planetary Science Letters 299, 299–309.
Melnick, D., Charlet, F., Echtler, H.P., De Batist, M., 2006. Incipient axial collapse of the Main Cordillera and strain partitioning gradient between the central and Patagonian Andes, Lago Laja, Chile. Tectonics 25, TC5004.
Menegatti, N.F., Massaferro, G.I., Fernández, M.I., Giacosa, R.E., 2014. Geología y geoquímica de los cuerpos básicos alcalinos al sur de los lagos Musters y Colhué Huapí, cuenca del Golfo San Jorge, Chubut. Revista de la Asociación Geológica Argentina 71 (4), 484–499 (in Spanish).
Min, K., Mundil, R., Renne, P.R., Ludwig, K.R., 2000. A test for systematic errors in $^{40}Ar/^{39}Ar$ geochronology through comparison with U/Pb analysis of a 1.1-Ga rhyolite. Geochimica et Cosmochimica Acta 64, 73–98.
Morata, D., de la Cruz, R., Suárez, M., 2005. The Bandurrias gabbro: late Oligocene alkaline magmatism in the patagonian Cordillera. Journal of South American Earth Sciences 18, 147–162.
Mpodozis, C., Nasi, C., Moscoso, R., Cornejo, P., Maksaev, V., Parada, M.A., 1985. El Cinturón Magmático del Paleozoico superior-Triásico de la Cordillera Frontal chilena entre los 28 y 31°S: 'estratigrafía' ígnea y marco tectónico, 35. Universidad de Chile, Comunicaciones, pp. 161–165 (in Spanish).
Mpodozis, C., Ramos, V., 1989. The Andes of Chile and Argentina. In: Ericksen, G., Cañas, M., Reinemund, J. (Eds.), Geology of the Andes and its Relation to Hydrocarbon and Mineral Resources. Circum-Pacific Council for Energy and Mineral Resources Earth Science Series, vol. 11, pp. 59–88.
Muñoz, J., Troncoso, R., Duhart, P., Crignola, P., Farmer, L., Stern, C.R., 2000. The relation of the mid-Tertiary coastal magmatic belt in south-central Chile to the late Oligocene increase in plate convergence rate. Revista Geologica de Chile 27, 177–203.
Nakamura, N., 1974. Determination of REE, Ba, Fe, Mg, Na and K in carbonaceous and ordinary chondrites. Geochimica et Cosmochimica Acta 38, 757–775. https://doi.org/10.1016/0016-7037(74)90149-5.
Navarrete, C.R., Gianni, G.M., Folguera, A., 2015. Tectonic inversion events in the western San Jorge Gulf Basin from seismic, borehole and field data. Journal of South American Earth Sciences 64, 486–497.
Niemeyer, R.H., 1975. Geología de la región comprendida entre el Lago General Carrera y el Río Chacabuco. Aisén. PhD Dissertation (unpublished). University of Chile, Departamento de Geología, p. 309 (in Spanish).
Niemeyer, H., Skarmeta, J., Fuenzalida, R., Espinoza, W., 1984. Hojas Península de Taitao y Puerto Aisén, vol. 60–61. Servicio Nacional de Geología y Mineria Carta Geológica de Chile, p. 80 (in Spanish).
Oncken, O., Hindle, D., Kley, J., Elger, K., Victor, P., Schemmann, K., 2006. Deformation of the central Andean upper plate system – facts, fiction, and constraints for plateau models. In: Oncken, O., Franz, G., Giese, P., Götze, H.J., Ramos, V., Strecker, M., Wigger, P. (Eds.), The Andes – Active Subduction Orogeny, vol. 513–535. Springer Earth Frontiers in Earth Sciences. ISBN: 978-3-540-24329-8.
Ortiz-Jaureguizar, E., Cladera, G.A., 2006. Paleoenvironmental evolution of southern south America during the cenozoic. Journal of Arid Environments 66, 498–532.
Orts, D.L., Folguera, A., Encinas, A., Ramos, M., Tobal, J., Ramos, V.A., 2012. Tectonic development of the North Patagonian Andes and their related Miocene foreland basin (41°30′–43°S). Tectonics 31, TC3012.
Palazzesi, L., Barreda, V., 2012. Fossil pollen records reveal a late rise of open-habitat ecosystems in Patagonia. Nature Communications 3, 1294.
Pankhurst, R.J., Weaver, S., Hervé, F., Larrondo, P., 1999. Mesozoic–cenozoic evolution of the north patagonian batholith in Aysén, southern Chile. Journal of the Geological Society of London 156, 673–694.
Pankhurst, R.J., Riley, T.R., Fanning, C.M., Kelley, S.P., 2000. Episodic silicic volcanism in Patagonia and the Antarctic peninsula: chronology of magmatism associated with the break-up of Gondwana. Journal of Petrology 41 (5), 605–625.
Pardo-Casas, F., Molnar, P., 1987. Relative motion of the Nazca (Farallón) and south American plates since late cretaceous time. Tectonics 6 (3), 233–248.
Paredes, J.M., Colombo, F., Foix, N., Allard, J.O., Nillni, A., Allo, M., 2008. Basaltic explosive volcanism in a tuff-dominated intraplate setting, Sarmiento Formation (middle eocene-lower Miocene), Patagonia Argentina. Latin American Journal of Sedimentology and Basin Analysis 15 (2), 77–92.
Paredes, J.M., Foix, N., Guerstein, R., Guler, M.V., Irigoyen, M., Moscoso, P., Giordano, S., 2015. A late eocene-early Oligocene transgressive event in the Golfo San Jorge basin: palynological results and stratigraphic implications. Journal of South American Earth Sciences 63, 293–309.
Parras, A., Dix, G.R., Griffin, M., 2012. Sr-isotope chronostratigraphy of Paleogene/Neogene marine deposits: Austral Basin, southern Patagonia (Argentina). Journal of South American Earth Sciences 37, 122–135.
Profeta, L., Ducea, M.N., Chapman, J.B., Paterson, S.R., Gonzales, S.M.H., Kirsch, M., Petrescu, L., DeCelles, P.G., 2015. Scientific Report. Quantifying Crustal Thickness Over Time in Magmatic Arcs, vol. 5.
Ramos, V.A., 1982. Geología de la región del Lago Cardiel, provincia de Santa Cruz. Revista de la Asociación Geológica Argentina 37, 23–49 (in Spanish).
Ramos, V.A., 1989. Andean foothills structures in northern Magallanes Basin, Argentina. AAPG Bulletin 73 (7), 887–903.
Ramos, V.A., 2005. Seismic ridge subduction and topography: foreland deformation in the Patagonian Andes. Tectonophysics 399 (1–4), 73–86.
Ramos, V., Kay, S.M., 1992. Southern Patagonian plateau basalts and deformation: backarc testimony of ridge collisions. Tectonophysics 205, 261–282.
Ramos, V.A., Ghiglione, M.C., 2008. Tectonic evolution of the patagonian Andes. Developments in Quaternary Sciences 11, 57–71.
Rapela, C.W., Spalletti, L.A., Merodio, J.C., Aragón, E., 1988. Temporal evolution and spatial variation of early tertiary volcanism in the Patagonian Andes (40°S–42°30′S). Journal of South American Earth Sciences 1, 75–88.

Ray, F.M., 1996. Stratigraphical and Structural Evolution of Tertiary Backarc Basins in Southern Chili. PhD Dissertation (Unpublished). University of Liverpool, p. 208.
Ré, G.H., Bellosi, E.S., Heizler, M., Vilas, J.F., Madden, R.H., Carlini, A.A., Kay, R.F., Vucetich, M.G., 2010. A geochronology for the Sarmiento Formation at gran Barranca. In: Madden, R.H., Carlini, A.A., Vucetich, M.G., Kay, R.F. (Eds.), The Paleontology of Gran Barranca: Evolution and Environmental Change through the Middle Cenozoic of Patagonia. Cambridge University Press, Cambridge, UK, pp. 46–60.
Renne, P.R., Knight, K.B., Nomade, S., Leung, K.-N., Lou, T.-P., 2005. Application of deuteron–deuteron (D–D) fusion neutrons to $^{40}Ar/^{39}Ar$ geochronology. Applied Radiation and Isotopes 62, 25–32.
Rivas, H., Bostelmann, E., Le Roux, J., Ugalde, R., 2015. Fluvial Facies and Architecture of Teh Late Middle Miocene, Mayoan, Deposits of Chilean Patagonia, vol. 1. XIV Congreso Geológico Chileno Actas, pp. 812–815.
Rodríguez Tribaldos, V., White, N.J., Robert, G.G., Hoggard, M.J., 2017. Spatial and temporal uplift history of south America from calibrated drainage analysis. Geochemistry, Geophysics, Geosystems 18, 2321–2353. https://doi.org/10.1002/2017GC006909.
Scalabrino, B., Lagabrielle, Y., Malavieille, J., Dominguez, S., Melnick, D., Espinoza, F., Rossello, E., 2010. A morphotectonic analysis of central Patagonian Cordillera: negative inversion of the Andean belt over a buried spreading center? Tectonics 29 (2), TC2010. https://doi.org/10.1029/2009TC002453.
Schmitz, M.D., Bowring, S.A., 2001. U-Pb zircon and titanite systematics of the Fish Canyon Tuff: an assessment of high-precision U-Pb geochronology and its application to young volcanic rocks. Geochimica et Cosmochimica Acta 65, 2571–2587.
Segemar (Servicio Geológico Minero Argentino), 1994. Mapa Geológico de la Provincia de Río Negro 1:750000, Republica Argentina. Ministerio de Economía, Obras y Servicios Públicos, Argentina (in Spanish).
Segemar (Servicio Geológico Minero Argentino), 1995. Mapa Geológico de la Provincia de Chubut 1:750000, Republica Argentina. Ministerio de Economía, Obras y Servicios Públicos, Argentina (in Spanish).
Sernageomín (Servicio Nacional de Geología y Minería de Chile), 2003. Mapa geológico de Chile, versión digital. Publicación Geológica Digital No. 4, CD-ROM, Versión 1.0, 2003, base geológica escala 1:1,000,000 (in Spanish).
Silver, P.G., Russo, R.M., Lithgow-Bertelloni, C., 1998. Coupling of South American and African plate motion and plate deformation. Science 279, 60–63.
Skarmeta, J., 1976. Evolución tectónica y paleogeográfica de los Andes Patagónicos de Aisén (Chile), durante el Neocomiano, vol. 1. I Congreso Geológico Chileno Actas, Santiago, pp. B1–B15 (in Spanish).
Sláma, J., Kosler, D.J., Condon, J.L., Crowley, A., Gerdes, J.M., Hanchar, M.S.A., Horstwood, G.A., Morris, L., Nasdala, N., Norberg, U., Schaltegger, B., Schoene, M.,N., Tubrett, M.J., 2008. Whitehouse Plesovice zircon - a new natural reference material for U-Pb and Hf isotopic microanalysis. Chemical Geology 249 (1–2), 1–35.
Stoenner, R., Schaeffer, O., Katcoff, S., 1965. Half-lives of argon-37, argon-39, and argon-42. Science 148, 1325–1328.
Suárez, M., De La Cruz, R., 2000. Tectonics in the eastern central patagonian Cordillera (45°30′–47°30′S). Journal of the Geological Society 157 (5), 995–1001.
Suárez, M., De la Cruz, R., Troncoso, A., 2000. Tropical/subtropical upper Paleocene–lower Eocene fluvial deposits in eastern central Patagonia, Chile (46°45′ S). Journal of South American Earth Sciences 13, 527–536.
Suárez, M., De La Cruz, R., Etchart, H., Márquez, M., Fanning, M., 2015. Síntesis de la Cronología Magmática Meso-Cenozoica de Patagonia Central, Aysén, Chile: edades U-Pb SHRIMP. XIV Congreso Geológico Chileno, Chile, pp. 789–792. ST4.
Sun, S. -S., McDonough, W.F., 1989. Chemical and isotopic systematics of oceanic basalts: implications for mantle composition and processes. Geological Society of London Special Publications 42, 313–345.
Süssenberger, A., Schmidt, S.T., Wemmer, K., Baumgartner, L.P., Grobéty, B., 2017. Timing and thermal evolution of fold-and-thrust belt formation in the Ultima Esperanza District. Geological Society of America Bulletin. https://doi.org/10.1130/B31766.1.
Thomson, S.N., Hervé, F., Stöckhert, B., 2001. Mesozoic Cenozoic denudation history of the Patagonian Andes (southern Chile) and its correlation to different subduction processes. Tectonics 20, 693–711.
Thomson, N., 2002. Late Cenozoic geomorphic and tectonic evolution of the Patagonian Andes between latitudes 42°S and 46°S: an appraisal based on fission-track results from the transpressional intra-arc Liquiñe-Ofqui fault zone. The Geological Society of America Bulletin 114, 1159–1173.
Troncoso, A., Suárez, M., De la Cruz, R., Palma-Heldt, S., 2002. Paleoflora de la Formacion Ligorio Márquez (XI Región, Chile) en su localidad tipo: paleobotánica, edad e implicancias paleoclimáticas. Revista Geologica de Chile 29 (1), 113–135 (in Spanish).
Ugarte, F.R.E., 1956. El Grupo de Río Zeballos en el flanco Occidental de la Meseta Buenos Aires (Provincia de Santa Cruz). Revista Asociación Geológica Argentina 11 (3), 202–216 (in Spanish).
Uliana, M.A., Biddle, K.T., 1988. Mesozoic-Cenozoic paleogeographic and geodynamic evolution of southern South America. Revista Brasileira de Geociências 18 (2), 172–190.
Valencia, V.A., Ruiz, J., Barra, F., Geherls, G., Ducea, M., Tittley, S.R., Ochoa-Landín, L., 2005. U–Pb zircon and Re–Os molybdenite geochronology from La Caridad porphyry copper deposit: insights for the duration of magmatism and mineralization in the Nacozari District, Sonora, Mexico. Mineralium Deposita 40, 175–191.
Varela, A.N., Poiré, D.G., Martin, T., Gerdes, A., Goin, F.J., Gelfo, J.N., Hoffmann, S., 2012. U-Pb zircon constraints on the age of the cretaceous mata Amarilla formation, southern Patagonia, Argentina: its relationship with the evolution of the Austral basin. Andean Geology 39, 359–379.
Williams, I.S., 1998. U-Th-Pb geochronology by ion microprobe. Reviews in Economic Geology 7, 1–35.
Wood, D.A., 1980. The application of a Th-Hf-Ta diagram to problems of tectonomagmatic classification and to establishing the nature of crustal contamination of basaltic lavas of the British Tertiary Volcanic Province. Earth and Planetary Science Letters 50, 11–30.
Yabe, A., Uemura, K., Nishida, H., 2006. Geological notes on plant fossil localities of the Ligorio Márquez Formation, central Patagonia, Chile. In: Nishida, H. (Ed.), Post-cretaceous Floristic Changes in Southern Patagonia, Chile. Chuo University, Tokyo, pp. 29–35.
Yanez, G., Cembrano, J., 2004. Role of viscous plate coupling in the late Tertiary Andean tectonics. Journal of Geophysical Research 109, B02407.